



Research paper

Novel dialkylphosphorylhydrazones: Synthesis, leishmanicidal evaluation and theoretical investigation of the proposed mechanism of action



Carolina Barbosa Brito da Matta ^a, Aline Cavalcanti de Queiroz ^a, Mariana Silva Santos ^a,
Magna Suzana Alexandre-Moreira ^a, Vinicius Tomaz Gonçalves ^{b, c},
Catarina de Nigris Del Cistia ^d, Carlos Mauricio R. Sant'Anna ^b, João Batista N. DaCosta ^{b, *}

^a LaFI – Laboratório de Farmacologia e Imunidade, Instituto de Ciências Biológicas e da Saúde, Universidade Federal de Alagoas, Maceió, AL, Brazil

^b Universidade Federal Rural do Rio de Janeiro, Departamento de Química, Rio de Janeiro, Seropédica, Brazil

^c CEFET/RJ – Centro Federal de Educação Tecnológica Celso Suckow da Fonseca, Itaguaí, RJ, Brazil

^d Universidade Federal Rural do Rio de Janeiro, Departamento de Matemática, Rio de Janeiro, Seropédica, Brazil

ARTICLE INFO

Article history:

Received 18 December 2014

Received in revised form

24 April 2015

Accepted 5 June 2015

Available online 9 June 2015

Keywords:

Dialkylphosphorylhydrazones

Leishmanicidal activity

Glycolytic pathway

Molecular docking

ABSTRACT

As part of a program to develop new drugs for the treatment of neglected diseases, new dialkylphosphorylhydrazones were synthesized and evaluated against the trypanosomatid parasites *Leishmania braziliensis* and *Leishmania amazonensis*. The synthesis of these compounds proved satisfactory with yields ranging from moderate to good. The most active compounds against *L. braziliensis* presented IC₅₀ values in the 10⁻² μM range, similar to that of the reference drug pentamidine. Two compounds, **4m** and **4n**, showed a significant dose dependent decrease in the infection index of *L. amazonensis* infected macrophages and caused a complete healing of nodules and ulcers when tested *in vivo* against *L. amazonensis*-infected mice, but the control of parasite burden at the inoculation site was statistically significant only in the case of treatment with **4n**. A target fishing (reverse docking) approach using molecular docking with 15 enzymes of *L. braziliensis* indicated that the probable target of the active compounds was hexokinase, the first enzyme of the glycolytic pathway.

© 2015 Elsevier Masson SAS. All rights reserved.

1. Introduction

Leishmaniasis is one of the world's most neglected diseases, with a major impact among the poorest individuals, mainly in developing countries. The number of leishmaniasis cases is increasing worldwide [1,2]. Leishmaniasis transmission is endemic in 98 countries and 3 territories on 5 continents. According to the World Health Organization, 350 million people are considered at risk of contracting this disease, and some 2 million new cases occur each year [1,3]. Each year approximately 58,000 cases of visceral leishmaniasis and 220,000 cutaneous cases are officially reported. However, it is thought that only approximately two-thirds of countries actually report incidence data, with the sparsest data from Africa [3].

One of the main problems in leishmaniasis treatment is the limited number of available drug options, along with the adverse effects they can cause, including death [4]. In addition, there are reports of treatment failures due to increased parasite resistance to the drugs of first choice, the antimonials [5,6]. Second-choice drugs, such as amphotericin B, pentamidine, paromomycin, and more recently, miltefosine, also have toxic effects, and their use requires hospital supervision [4,7]. Therefore, there is an urgent need for the development of safer and more effective drugs against this parasite.

Screening tests implemented with a series of new dialkylphosphorylhydrazones (DAPH) synthesized by our group were indicative of promising activity profiles against *Trypanosoma cruzi* and *Leishmania amazonensis* [8]. New compounds were then synthesized and added to the series. In the present work, we show the synthesis of the entire DAPH series and a detailed evaluation of the compounds' leishmanicidal activity against *L. amazonensis* and *Leishmania braziliensis* in comparison with known leishmanicidal agents. Although the information available from these *in vivo* tests

* Corresponding author.

E-mail address: dacosta@ufrrj.br (J.B.N. DaCosta).

is essential for the identification of new leishmanicidal agents, an understanding of the observed effects is a prerequisite for improving the selectivity and potency of the investigated compounds. In an attempt to identify probable targets for the active compounds prepared in the present work, we also implemented a strategy based on molecular docking of the compounds into a set of candidate target enzymes.

The presence of the (R'O)₂P(O)NHR group in DAPH suggests that these molecules could act as inhibitors of enzymes that have, as substrates, molecules containing the (R'O)₂P(O)OR group. There are a huge number of such enzymes, so the target identification procedure should be based on some criteria to reduce the number of possibilities to be explored. Some parasite enzymes have been shown to be inhibited by phosphorous-containing molecules, such as farnesyl pyrophosphate synthase (FPPS) [9,10] and hexokinase (HK) [11], an enzyme of glycolysis metabolic pathway in which glucose is converted into pyruvate and the free energy released is used to form the high-energy compounds ATP and NADH. In addition to FPPS and the enzymes of the glycolytic pathway, promising targets also include the enzymes of the pentose phosphate pathway (PPP), which serves to convert glucose-6-phosphate to ribose-5-phosphate. The PPP has been proposed to have crucial roles in the protection of trypanosomatids against oxidative stress, as well as in the production of nucleotide precursors [12]. Each of the enzymes of the PPP has been identified and specific activities measured for one of the Leishmania species, *Leishmania Mexicana* [13].

2. Results and discussion

2.1. Synthesis of the dialkylphosphorylhydrazones

The synthesis of the dialkylphosphites (**1**) and dialkylphosphorylhydrazines (**2**) were performed using the synthetic route previously used by our research group [14–18], according to the synthetic route shown in Scheme 1.

The synthesis of the new DAPH (**4a–o**) occurred through a condensation reaction, catalyzed in an acidic medium, between the respective dialkylphosphorylhydrazines (**2**) and different aldehydes (**3**) at room temperature, as shown in Scheme 2.

The infrared spectra of the DAPH synthesized show the characteristic absorption bands. The main absorption bands correspond to the stretching frequencies of the P=O, P–O–C and C=N bonds. In pentavalent phosphorus compounds containing a bond between a phosphorus atom and a nitrogen atom, the stretching frequency range of the P=O bond is generally from 1198 to 1274 cm⁻¹ [19], the P–O–C bond absorbs in the 950–1018 cm⁻¹ range, and the C=N bond has a stretching frequency in the 1580–1690 cm⁻¹ range [20]. These frequencies were observed for all products, which confirm the expected reactions.

In the ¹H-NMR analyses, two characteristic signals confirm that the DAPH were obtained. These signals correspond to the iminic hydrogen –NHN=CH–Ar, with a chemical shift (δ) in the range of

7.88–8.26 ppm; and to the phosphoramidic hydrogen, P(O)NH, with a chemical shift in the 9.74–10.21 ppm range and showing a doublet signal with a coupling constant ranging between 27 and 31 Hz. The literature reports that this coupling occurs between 23 and 53 Hz [21]. Compounds **4i** and **4j** also presented an additional doublet in the region approximately 12.8 ppm, with a coupling constant of approximately 34 Hz, which is characteristic of an intramolecular hydrogen bond.

NOEDIF experiments were used to determine the configuration of the synthesized compounds. The results clearly show, according to ¹H-NMR spectroscopy, that all molecules have the *E* configuration, except for compounds **4i** and **4j** which were obtained as a diastereoisomeric mixture with *E/Z* ratio of 80:20 and 85:15, respectively.

In the ¹³C NMR spectrum of DAPH, the signal that characterizes these compounds is related to the iminic carbon, (–NHN=CH–Ar), which has a chemical shift in the 136–145 ppm range and is observed as a doublet because it is coupled with the phosphorus atom, with a coupling constant in the 18–21 Hz range. The same feature can be observed with the alkoxide groups, (RCH_xO)₂P(O)–, where the methylene hydrogens, neighbors to the ester oxygen atoms, have chemical shifts in the range from 3.7 to 4.5 ppm.

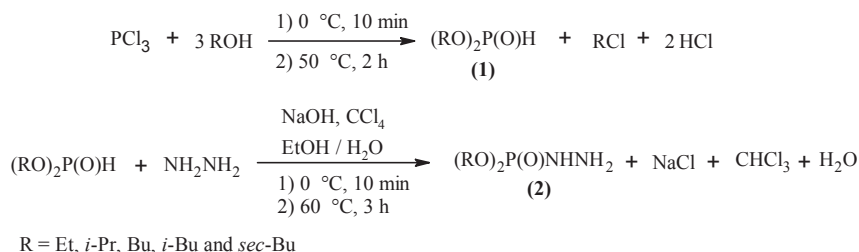
2.2. Biological evaluation

An initial screening was carried out to evaluate and compare the in vitro leishmanicidal profiles of the 18 DAPH and 2 standard drugs, miltefosine and pentamidine, against the promastigote forms of *L. braziliensis* and *L. amazonensis*. The maximum effects and the IC₅₀ values (concentrations causing 50% inhibition of growth of the promastigotes) were used as the parameters for leishmanicidal activity (Table 1).

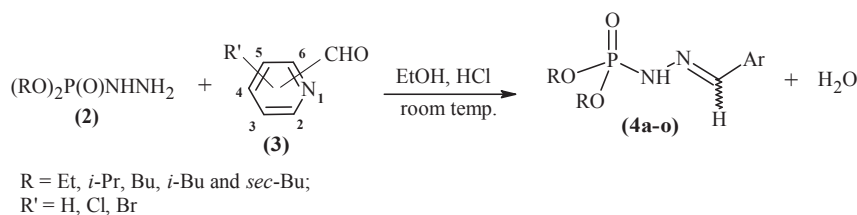
After 48 h of incubation, most of the compounds were significantly active against *L. braziliensis*. Among these, those that showed efficacy greater than 70% were as follows: **4b** (IC₅₀: 5.1 ± 0.5 μM), **4d** (IC₅₀: 0.06 ± 0.0 μM), **4f** (IC₅₀: 5.4 ± 0.2 μM), **4g** (IC₅₀: 0.4 ± 0.3 μM), **4h** (IC₅₀: 40.7 ± 3.5 μM), **4j** (IC₅₀: 0.06 ± 0.0 μM), **4m** (IC₅₀: 3.6 ± 0.3 μM), **4n** (IC₅₀: 5.2 ± 0.7 μM) and **4o** (IC₅₀: 0.03 ± 0.02 μM).

However, not all of these compounds were active against *L. amazonensis* as they were for *L. braziliensis*. The compounds **4b**, **4d**, **4g** and **4h** showed high specificity against the *L. braziliensis* species. The compounds were active against *L. amazonensis* with efficacies greater than 70% were as follows: **4f** (IC₅₀: 53.3 ± 2.9 μM), **4j** (IC₅₀: 6.2 ± 1.7 μM), **4m** (IC₅₀: 26.3 ± 2.0 μM), **4o** (IC₅₀: 26.0 ± 7.8 μM) and **4n** (IC₅₀: 0.001 ± 0.1 μM). Compound **4n** was as effective as miltefosine (IC₅₀: 3.4 ± 0.4 μM) and pentamidine (IC₅₀: 1.8 ± 1.1 μM) and was approximately 2000 times more potent than these standard drugs.

An important criterion in the search for new substances with leishmanicidal activity is that they should not be toxic to mammalian cells, a requirement for further clinical development. Therefore, the cytotoxic potential of these substances on J774



Scheme 1. Synthetic route for dialkylphosphites (**1**) and dialkylphosphorylhydrazines (**2**).



Scheme 2. Synthetic route for DAPH(4a-o).

Table 1

Activity of DAPH against promastigote forms of *L. braziliensis* and *L. amazonensis*.

Substance	<i>L. braziliensis</i>		<i>L. amazonensis</i>	
	IC ₅₀ (μM)	Efficacy (%)	IC ₅₀ (μM)	Efficacy (%)
Miltefosine	0.7 ± 0.6	84.5 ± 0.3	3.4 ± 0.4	96.3 ± 0.3
Pentamidine	0.06 ± 0.02	95.7 ± 0.5	1.8 ± 1.1	93.8 ± 0.7
4a	>100	NA	>100	NA
4b	5.1 ± 0.5	77.2 ± 4.2	99.3 ± 0.7	45.5 ± 3.2
4c	>100	NA	>100	NA
4d	0.06 ± 0.0	84.2 ± 2.6	>100	NA
4e	>100	NA	>100	NA
4f	5.4 ± 0.2	87.9 ± 1.1	53.3 ± 2.9	85.6 ± 0.5
4g	0.4 ± 0.3	75.9 ± 6.6	>100	NA
4h	40.7 ± 3.5	81.6 ± 0.4	83.3 ± 11.6	52.8 ± 5.6
4i	7.5 ± 0.8	62.1 ± 3.4	>100	NA
4j	0.06 ± 0.0	76.3 ± 8.7	6.2 ± 1.7	69.5 ± 4.2
4k	0.7 ± 0.1	56.3 ± 2.7	>100	NA
4l	>100	NA	98.3 ± 1.2	40.7 ± 6.1
4m	3.6 ± 0.3	92.2 ± 0.4	26.3 ± 2.0	93.8 ± 0.3
4n	5.2 ± 0.7	80.1 ± 2.6	<0.001	95.3 ± 0.4
4o	0.03 ± 0.02	74.1 ± 0.3	26.0 ± 7.8	92.4 ± 0.1

Data are reported as the mean ± standard error of the mean, S.E.M. Differences with an ***p* < 0.01 were considered significant in relation to the 0.1% DMSO group. IC₅₀ is the concentration required to give 50% inhibition; NA: compound is not active.

macrophages (murine cell line) was determined by the colorimetric MTT method, which was originally described by Mossmann [22]. In this assay, all substances, including the reference drugs miltefosine and pentamidine, showed low cytotoxicity against J774 macrophages with LC₅₀ values >100 μM, except for **4o**, which was toxic to approximately 20.5 ± 0.1% of the treated cells. It is important to stress that the reference drug pentamidine was toxic to 28.8 ± 0.1% of the cells at 100 μM.

From these results, some substances have been selected for tests on intracellular amastigotes and *in vivo* model. The selection criteria took into account the potency, the efficacy against both species and the cytotoxicity of each compound. Among the substances tested, only **4f**, **4j**, **4m**, **4o** and **4n** showed activity against both species with efficacies greater than 70%. However, **4m** and **4n** best fulfilled the requirements and, therefore, have been chosen for the subsequent tests.

With respect to activity against intracellular amastigotes 48 h post infection, the results showed that the treatment with **4m** and **4n** resulted in a significant (*p* < 0.01), dose dependent decrease in infection index of *L. amazonensis* infected macrophages with an inhibition of 99.9% and 97.9% (100 μM), respectively (Fig. 1A). Infected cultures were also treated with the highest concentration of DMSO used for substances solubilization (0.01%) and the viability and infection of macrophages were not reduced (data not shown). Miltefosine was also significantly different compared to the control (*p* < 0.01), with an inhibition of 100%.

The average of the number of parasites per macrophage and the percentage of infected macrophages, which influence the calculation of the index of infection, were also analyzed (Fig. 1B). The mean number of intracellular parasites per macrophage decreased

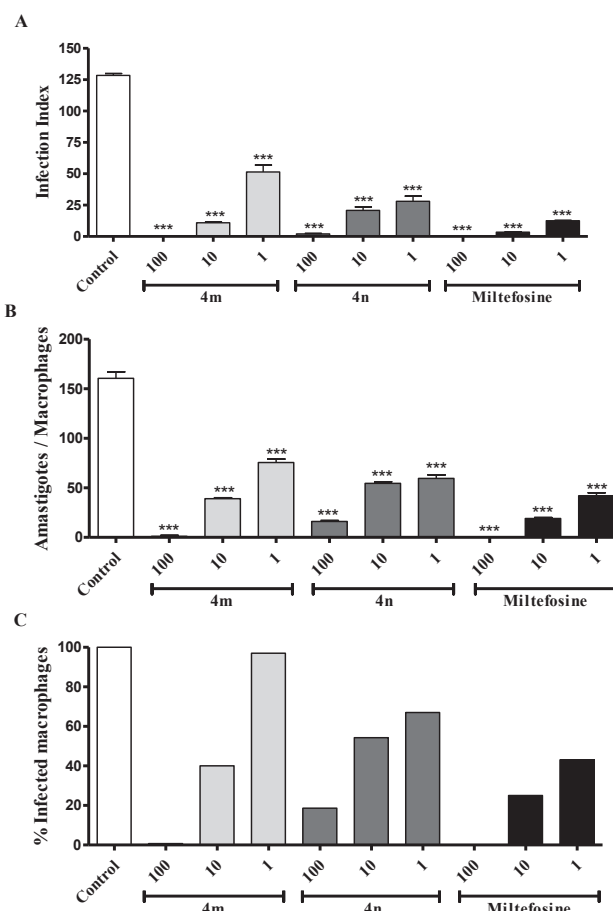


Fig. 1. Activity of **4m**, **4n** and miltefosine against intracellular parasites 48 h post infection. A: infection index. B: number of parasites per macrophages infected. C: percentage of macrophages infected. Data are reported as the mean ± standard error. Differences with an ****p* < 0.01 were considered significant in relation to the control group.

compared to the control after treatment with **4m** and **4n** (*p* < 0.01). The percentage of infected macrophages (Fig. 1C) was also reduced by both substances, with exception of **4m** at 1 μM, which showed no significant difference compared to the control. **4m** and **4n** showed higher percentages of inhibition of infection at 100 μM (99.9 and 82.2%, respectively).

Using an established mouse model of cutaneous leishmaniasis that mimics human leishmaniasis [23], BALB/c mice were infected in the ear dermis with 10⁵ stationary phase *L. amazonensis* promastigotes, and lesion development and parasite burden were quantified. Infected mice were treated orally for 28 consecutive days with **4m** or **4n** or standard drug. The untreated group was used as a control and resulted in an average lesion size of 0.2831 mm (S.E.M = 0.1022). The treated groups had significantly

reduced lesion size in the ear, the averages being 0.0527 mm (S.E.M = 0.03482) and 0.0804 mm (S.E.M = 0.0392) in **4m**- and **4n**-treated groups, respectively. These results were similar to the miltefosine group, with an average lesion size of 0.0231 mm (S.E.M = 0.0021) (Fig. 2).

To investigate if there was a correlation between lesion development and parasite replication, parasite load was estimated at both the inoculation site and the draining lymph nodes. In the ear dermis (Fig. 3A), **4n** treatment controlled parasite burden in a statistically significant manner, corroborating the therapeutic improvement in lesions of the ears. However, **4m** was not able to reduce the parasite load, although it caused a reduction in the ear lesion.

However, **4m** and **4n** did not reduce the parasite burden in the draining lymph node (Fig. 3B). This result indicates that either the dose (30 mg/kg/day) was not sufficient to control the infection systemically or, in addition to leishmanicidal activity, such compounds also have anti-inflammatory activity. Parasite load was reduced at the inoculation site and in the draining lymph nodes after miltefosine treatment.

3. Molecular modeling

3.1. Homology models

Table 2 presents details about models of *L. braziliensis* and *L. amazonensis* enzymes: PDB code and resolution of the template;

sequence identity; GMQE (Global Model Quality Estimation), which is a quality estimation that is expressed as a number between zero and one, reflecting the expected accuracy of a model built with that alignment and its template [24]; QMEAN4, which is a composite scoring function for the estimation of the global and local model quality, consisting of four structural descriptors [25]; and the quaternary structure information for the models. Ramachandran plots were generated with the Rampage server [26] and are available as [supplementary material](#).

The sequence identities between the models and their templates were above 30%, with the exception of the ENO and PGM enzymes. The Ramachandran plots for ENO and PGM enzyme models presented 4.7% and 5.5% residues in the outlier region, respectively, whereas all of the remaining models have at least 98% of their residues in the favored and/or allowed regions. The resulting models obtained for these two enzymes presented GMQE values lower than 0.5 and very low values of QMEAN4. Attempts to improve the models' quality were unsuccessful, and these enzymes were excluded from the subsequent target fishing procedure. As seen in Table 2, excluding PGM, a monomer resulted from the modeling procedure in five cases. This was not a problem for molecular docking in RPE, TAL, HK, and PGK, because the active site of these enzymes involves residues of a single chain, but this was not the case for RPI. Analysis of the tetrameric co-crystal structure of *Trypanosoma cruzi* RPI and its substrate (PDB code 3K7S) revealed that the active site of RPI shares residues from two adjacent chains.

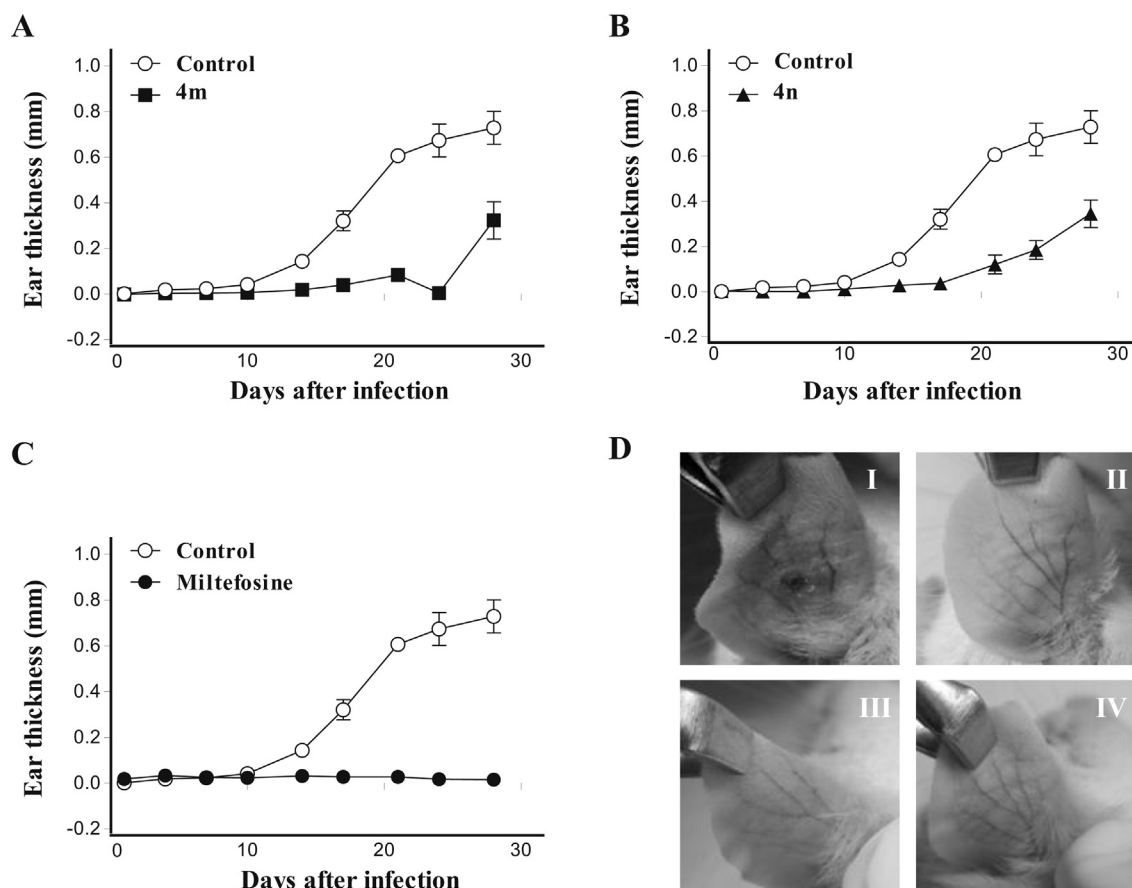


Fig. 2. *In vivo* leishmanicidal effect of **4m** and **4n** in BALB/c *Leishmania*-infected mice. Mice were infected with 10^5 *L. amazonensis* promastigotes, and the course of lesion development was monitored for 28 days during treatment with **4m** (A), **4n** (B) and miltefosine (C). Lesion size (mm) is expressed as the mean \pm SEM of a representative experiment ($n = 5$ mice in each experimental group) (Unpaired t-test, 5 weeks, $***p < 0.0001$). (D) Images of lesions after the end of treatment of BALB/c mice infected with *L. amazonensis*. In the vehicle control group (I), the lesions showed an intense swelling and were ulcerated. In groups treated with miltefosine (II), **4m** (III) and **4n** (IV) at doses of 30 mg/kg/day, the pictures reveal a complete healing of the nodules and ulcers.

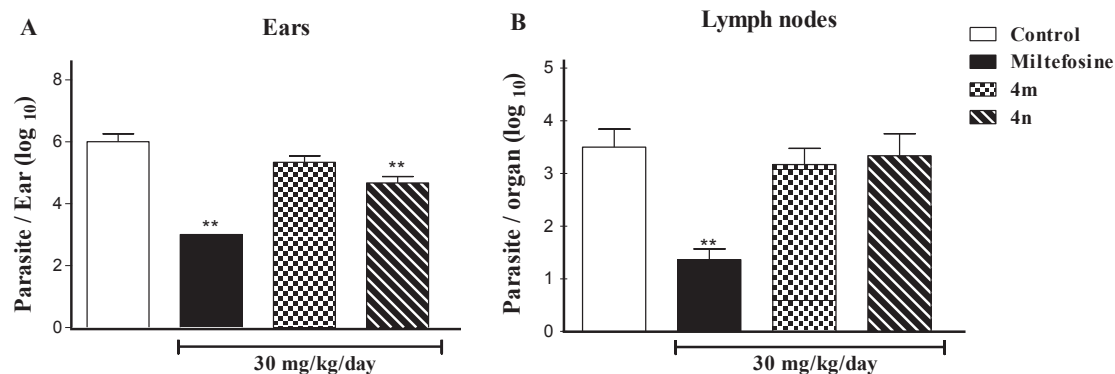


Fig. 3. Parasite load in the ear and draining lymph node were determined at 4 weeks post-infection via a limiting dilution assay. (A) Ear parasite load data (normal distribution following log transformation) represent the mean \pm SEM ($n = 5$) (Dunnett's test, $**p = 0.05$). (B) Lymph node parasite load data were not normally distributed, even after log transformation, and are expressed as the median \pm SEM ($n = 5$) (Dunnett's test, $**p = 0.05$).

Table 2
L. braziliensis and *L. amazonensis* enzyme models.

Enzyme model	PDB code of template	Template resolution	Sequence identity	GMQE	QMEAN4	Quaternary structure of model
6PGDH ^a	1pgj(A)	2.82	72.54	0.92	-1.76	dimer
G6PDH ^a	4e9i(A)	2.85	65.89	0.77	-2.20	tetramer
RPI ^a	3k7p(A)	1.40	49.36	0.81	-1.87	monomer
RPE ^a	1h1y(A)	1.87	45.98	0.71	-2.10	monomer
TAL ^a	1f05 (A)	2.45	59.43	0.80	-2.84	monomer
TKT ^a	1r9j(A)	2.22	84.95	0.96	-0.15	dimer
HK ^a	3o4w(A)	1.61	37.59	0.71	-5.50	monomer
PGI ^a	1t10 (A)	2.35	88.81	0.96	-1.22	dimer
PFK ^a	2hig(A)	2.40	70.81	0.81	-1.00	tetramer
FBPA ^a	1epx(A)	1.80	91.87	0.98	-0.28	tetramer
TPI ^a	1amk(A)	1.83	88.84	0.98	-0.29	dimer
GPDH ^a	1i32 (C)	2.60	91.39	0.99	-0.31	tetramer
PGK ^a	16pk (A)	1.60	48.33	0.61	-4.08	monomer
PGM ^a	3f3k(A)	1.75	21.43	0.21	-10.22	monomer
ENO ^a	1iyx(B)	2.80	23.33	0.47	-18.22	dimer
PYK ^a	3pp7(A)	2.35	92.49	0.99	0.81	tetramer
FPPS ^a	3dyh(A)	1.94	62.12	0.81	-2.06	dimer
6PGDH ^b	1pgj(A)	2.82	72.38	0.92	-1.76	dimer
G6PDH ^b	4e9i(A)	2.85	65.16	0.77	-2.77	tetramer

^a *L. braziliensis*.

^b *L. amazonensis*.

To obtain a structure with a complete active site, we constructed a dimer with Swiss PDB-Viewer 4.01 by superposition of the monomeric model of *L. braziliensis* RPI with both chains of its dimeric template 3K7P. This dimeric model of *L. braziliensis* RPI, after energy minimization with GROMOS96 [27], presented a very low RMSD value (0.34 Å) when superimposed on 3K7P and was used for the subsequent docking study.

3.2. Molecular docking

The identification of the biochemical target of a group of compounds with experimentally determined bioactivities is a very difficult task. In fact, the observed *in vivo* effects can involve several biochemical targets simultaneously. Together with virtual screening approaches to identify candidate ligands for a specific target, the availability of a great number of 3D structures of proteins has stimulated the development of theoretical methodologies to search for the targets of bioactive ligands, a process called target fishing or reverse docking [28,29]. The method is particularly useful in cases where purified enzymes are not available in sufficient

amounts to apply experimental procedures, such as in the case of the many parasites associated with neglected diseases. We explored molecular docking methodology as a way to implement small-scale target fishing for the active compounds identified in the bioassays. To improve the chances of identifying the best docking solution for each enzyme, docking runs were performed as duplicates, and the solution with the highest fitness score in each case was selected for further analysis. GOLD fitness scores are dimensionless, but the scale of the score provides a guide as to how good a ligand pose is - the higher the score for a specific function, the better the docking result is likely to be.

The limitations of scoring functions to produce data that correlate with activity data is well known, but docking programs have demonstrated the ability to identify active compounds from a pharmaceutically relevant pool of decoy compounds [30]. Based on the IC₅₀ data (Table 1), it can be concluded that the most active compounds against *L. braziliensis* were **4d**, **4j** and **4o**, all presenting activities in the 10⁻² μM range. Therefore, our analysis was focused on identifying enzymes for which these three compounds presented an improved binding profile in comparison with the remaining molecules, as measured by their docking fitness scores. As seen in Tables 3 and 4, **4d**, **4j** and **4o** were classified as the three best ligands only in the case of the docking procedure with *L. braziliensis* HK as the target. HK was validated as a target for

Table 3

ChemPLP score results from docking into *L. braziliensis* and *L. amazonensis* PPP enzymes.^a

	<i>L. braziliensis</i>							<i>L. amazonensis</i>	
	6PGL	6PGDH	G6PDH	RPE	RPI	TAL	TKT	6PGDH	G6PDH
4a	47.7	45.0	45.2	48.6	43.6	43.6	50.8	45.9	44.3
4b	51.4	55.1	55.8	51.5	54.0	46.7	58.7	53.9	52.1
4c	47.7	46.5	46.0	48.5	45.9	48.1	56.0	47.7	46.3
4d	50.2	53.7	48.3	49.5	50.9	46.3	57.8	53.1	48.7
4e	44.1	44.1	46.2	53.3	45.8	42.0	44.9	45.4	41.5
4f	50.3	54.4	53.8	55.5	55.9	46.6	61.3	56.3	52.6
4g	47.0	48.2	45.0	45.2	45.0	49.3	58.2	50.7	42.6
4h	47.1	55.7	48.3	50.5	54.5	48.3	57.0	61.3	49.4
4i	42.6	46.5	43.8	50.0	41.9	41.4	47.0	46.2	44.1
4j	49.9	55.9	53.7	51.9	52.2	44.5	60.6	55.8	49.1
4k	43.7	46.4	43.2	42.6	42.7	46.4	47.5	46.4	42.2
4l	46.8	54.1	47.8	48.8	50.2	43.4	58.4	54.4	47.2
4m	42.8	50.3	45.0	40.2	48.1	48.5	52.3	53.2	48.2
4n	48.4	51.9	47.3	45.4	50.6	40.0	55.8	54.4	50.2
4o	41.3	47.6	48.5	35.8	43.8	44.1	52.4	51.9	45.2

^a Bold values indicate the three highest score values.

Table 4
ChemPLP score results from docking into *L. braziliensis* glycolysis and FPPS enzymes.^a

	HK	PGI	PFK	FBPA	TPI	GPDH	PGK	PYK	FPPS
4a	42.6	43.6	47.4	51.3	51.3	45.8	45.5	48.8	68.4
4b	49.6	53.9	62.6	58.4	58.6	57.2	53.1	57.9	78.8
4c	44.3	45.6	52.8	55.9	50.2	49.2	44.5	50.0	70.0
4d	51.4	51.0	59.8	59.0	57.4	56.7	50.7	56.6	67.9
4e	40.9	45.5	48.6	53.4	51.3	48.2	42.3	47.3	65.5
4f	51.4	56.0	61.3	63.1	60.1	57.3	51.6	56.0	90.6
4g	45.2	45.9	52.3	57.6	53.3	49.9	43.6	48.5	69.7
4h	49.8	50.4	59.7	59.9	57.6	56.3	49.3	54.0	78.7
4i	45.1	43.6	48.4	52.8	53.7	47.2	41.8	49.9	66.5
4j	54.2	52.6	61.7	58.7	60.9	59.7	52.5	53.7	76.3
4k	44.5	40.6	52.9	57.6	56.4	50.6	44.6	49.9	70.6
4l	50.6	47.6	58.6	56.0	53.2	58.8	46.1	53.3	69.5
4m	50.5	49.4	60.6	60.2	56.4	56.3	49.9	49.6	69.7
4n	49.3	51.3	64.3	54.5	62.3	56.0	48.4	53.8	68.2
4o	52.9	43.2	61.7	53.8	62.1	54.8	49.6	53.0	66.6

^a Bold values indicate the three highest score values.

another trypanosomatid, *T. cruzi*, in experiments involving some phosphorus-containing compounds [11,31]. Comparison of *L. braziliensis* (UniProtKB/Swiss-Prot code A4HBM3) and *T. cruzi* (Q4DQ27) HK sequences with the SIM alignment tool [32] revealed

that the overall identity between the two sequences is 65.8% (471 residues), which is suggestive that similar inhibition mechanisms may operate in HK from both species.

In the case of *L. amazonensis*, the inhibition profile was not the same as with *L. braziliensis*, and there is only one compound with activity in the submicromolar range, **4n**. The docking analysis was, in this case, unfortunately limited to a pair of enzymes, and **4n** was not classified by the docking procedure as the best ligand with any of these enzymes. Therefore, it was not possible to identify the probable biochemical target for this *Leishmania* species.

After identification of HK as the most probable target of the bioactive DAPH against *L. braziliensis*, we compared the interaction profiles of the best poses obtained for the most active compounds with the co-crystallized structure of the HK reaction product, glucose-6-phosphate (G6P) (PDB code 1CZA). As an example, Fig. 4A and B presents the superposition of the structure 1CZA with the complex between compound **4d** and *L. braziliensis* HK. It can be observed that compound **4d** can occupy the same site as G6P in HK, but one of its *iso*-butyl groups is inserted into an adjacent binding site, which is occupied by a glucose molecule in the co-crystal structure. It can also be observed that the G6P binding site is smaller and the neck connecting both sites is narrower in the human enzyme (Fig. 1A) than in the *L. braziliensis* enzyme (Fig. 1B).

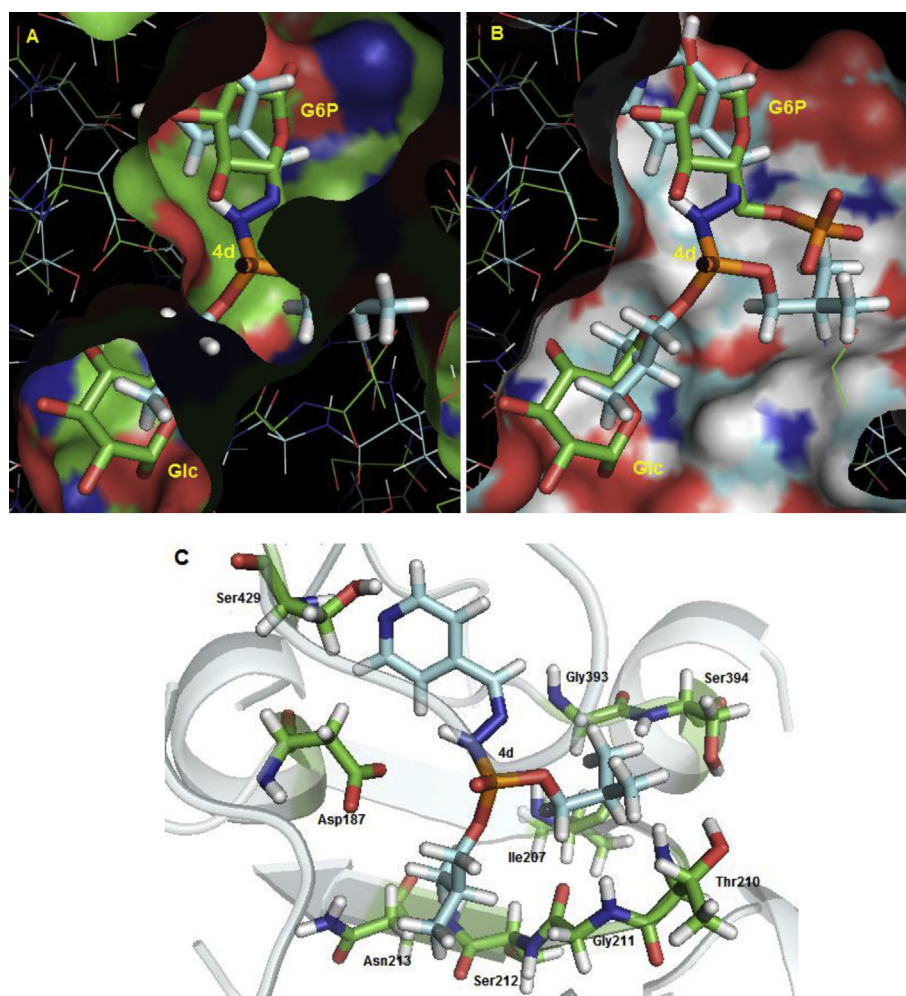


Fig. 4. (A and B) Superposition of the best-ranked pose of DAPH **4d** (carbon atoms in cyan, stick representation) into *L. braziliensis* hexokinase (carbon atoms in cyan) with the co-crystal structure of human hexokinase (carbon atoms in green) containing glucose-6-phosphate (G6P, stick representation) and glucose (Glc, stick representation) (PDB code 1CZA). In **A** it is shown the molecular surface of human hexokinase and in **B** the molecular surface of *L. braziliensis* hexokinase. (C) *L. braziliensis* hexokinase residues (carbon atoms in green) interacting with **4d** (carbon atoms in cyan). Color code for the remaining atoms: oxygen, red; nitrogen, blue; hydrogen, white; phosphorus, orange. Figures were generated with PyMOL. (For interpretation of the references to colour in this figure legend, the reader is referred to the web version of this article.)

This observation suggests the **4d** molecule would probably have difficulties to be accommodated in the human HK enzyme, which is indicative of some level of selectivity of **4d** for the parasite enzyme. Fig. 1C presents the *L. braziliensis* HK amino acid residues interacting with **4d**, including residues from G6P and glucose binding sites. Four of these residues have correspondent residues in the human enzyme that are interacting directly with G6P Asp187 (Asp209 in human HK), Thr210 (Thr232), Ser394 (Ser415) and Ser429 (Ser449).

4. Conclusion

The synthesis of new dialkylphosphorylhydrazones proved satisfactory, with yields ranging from moderate to good. An excellent advantage of these compounds is that they have a fairly simple synthesis methodology. The compounds had their *in vitro* leishmanicidal profile evaluated, and some active compounds could be identified with efficacy greater than 70% against *L. braziliensis* (**4b**, **4d**, **4f**, **4g**, **4h**, **4j**, **4m**, **4n**, and **4o**) and against *L. amazonensis* (**4f**, **4j**, **4m**, **4n**, and **4o**). The compounds with the greatest efficacy against both species, **4m** and **4n**, were tested *in vivo* against *L. amazonensis*-infected mice. Both of the compounds completely healed the nodules and ulcers, but control of parasite burden at the inoculation site was statistically significant only in the case of **4n** treatment.

Comparing the corresponding IC₅₀ values, the only compounds with IC₅₀ against *L. braziliensis* in the 10⁻² μM range (the same range for pentamidine activity) were **4d**, **4j**, and **4o**. Compound **4n** was the only one with an IC₅₀ value in the submicromolar range against *L. amazonensis*, which was even lower than that for the reference compounds pentamidine and miltefosine. A target fishing procedure based on docking methodology using 15 different enzymes from *L. braziliensis* and two from *L. amazonensis* was implemented to identify probable biochemical targets for the active compounds. After comparison with the IC₅₀ values, it was concluded that hexokinase is the most probable target in *L. braziliensis*, but it was not possible to identify a target for *L. amazonensis* because of the limited number of candidate enzymes available for this species.

5. Experimental section

5.1. Chemistry

All solvents used in reactions and purification methods were distilled prior to use and, when necessary, treated and dried according to the usual methods described in the literature [33]. Thin layer chromatography was performed using 0.2 mm-thick, aluminum-backed plates containing Kieselgel 60 F254, and visualized under UV light at 254 nm.

The devices used for the characterization of the compounds were as follows: (a) Perkin–Elmer infrared spectrometer, model 1600 FT. The spectra were obtained using a film on NaCl cells in the case of liquid samples, and KBr pellets in the case of solid samples. The absorptions were measured in reciprocal centimeters (cm⁻¹); (b) gas chromatograph coupled to a mass spectrometer, Varian Saturn model 2000. The analysis conditions were VF-5ms column (30 × 0.25 × 0.25 mm), oven temperature 150–290 °C/10 °C/min, injector 270 °C, MS trap 220 °C, manifold 60 °C, transfer line 250 °C, EI ionization (70 eV); (c) NMR spectra were performed on a Bruker AC 200 spectrometer (¹H NMR: 200 MHz, ¹³C NMR: 50.3 MHz, ³¹P NMR: 81.0 MHz) and Bruker AVANCE II 400 spectrometer (¹H NMR: 400 MHz, ¹³C NMR: 100.6 MHz, ³¹P NMR: 161.9 MHz). The spectra were obtained using tetramethylsilane (TMS) or the solvent itself as a reference for ¹H and ¹³C spectra. For ³¹P spectra, 85% phosphoric

acid was used as the external reference. In each case, the deuterated solvents are specified, the chemical shifts are measured in ppm and the coupling constants are in Hertz (Hz).

5.2. General procedure

In a 50 mL flask, the dialkylphosphorylhydrazine and the specific aldehyde in a 1:1 M ratio, ethanol, and three drops of 37% hydrochloric acid as the reaction catalyst were added. The reaction mixture was stirred at room temperature (25 °C) for approximately 4 h. At the end of the reaction, sodium bicarbonate (10%) was added to neutralize the reaction mixture. The resulting solution was transferred to a beaker containing 20 mL of cold distilled water in an ice bath. After approximately 20 min, a solid material was observed that was subsequently filtered and dried at room temperature. Compounds that did not precipitate in water were transferred to a separatory funnel with the aid of an appropriate amount of methylene chloride. After separation of the resulting layers, anhydrous magnesium sulfate was added to the organic phase for complete removal of residual water. Filtration was carried out for removal of the drying agent, and the solvent was evaporated under vacuum, after which an oily product was obtained.

6. Characterization of the products

6.1. Phosphorohydrazidic acid, *N'*-[(1*E*)-4-pyridinylmethylene]-diethyl ester (**4a**)

Aspect: orange oil. **yield:** 53%. **IR (NaCl):** 3425.7 (st, NH); 3149.6 (st, CH_{aromatic}); 2985.7, 2925.9 and 2821.7 (st_{ass}, CH₃ and CH₂); 1597.0 (st, C=N); 1475.5 (δ_{ass}, CH₂ and CH₃); 1407.9 (δ_{sim}, CH₃); 1240.1 (st P=O); 1163.0 (st, P–N); 1031.8 (st, P–O–C). **NMR ¹H (DMSO):** 9.95 [d, (P–N–H), J_{HP} = 29.0 Hz, 1H]; 8.56 [d, (H₂ and H₆), J_{ortho} = 6.27 Hz, 2H]; 7.89 [s, (N=CH), 1H]; 7.48 [d, (H₃ and H₅), J_{ortho} = 6.27 Hz, 2H]; 4.03 [m, (CH₃CH₂OP), 4H]; 1.23 [t, (CH₃CH₂OP), J_{HH} = 7.41 Hz, 6H]. **NMR ¹³C (DMSO):** 150.13 [s, (C₂ and C₆), 2C]; 141.76 [s, (C₄), 1C]; 141.46 [d, (N=C), J_{CP} = 20.35 Hz, 1C]; 120.23 [s, (C₃ and C₅), 1C]; 62.57 [d, (CH₂OP), J_{CP} = 5.30 Hz, 2c]; 16.06 [d, (CH₃CH₂OP), J_{CP} = 6.26 Hz, 2c]. **NMR ³¹P (DMSO):** 1.33 [dq, (P–N–H), J_{HP} = 29.35 Hz, (CH₂OP), J_{HP} = 7.91 Hz]. **m/z:** 45(8%), 81(61%), 98(100%), 126(87%), 133(3%), 153(22%), 184(3%), 200(2%), 228(1%), 258(3%). HR-MS(ESI) calc. for C₁₀H₁₆N₃O₃P (M)⁺: 257.092928, found: (M + H)⁺: 258.100204, (M + Na)⁺: 280.082149.

6.2. Phosphorohydrazidic acid, *N'*-[(1*E*)-4-pyridinylmethylene]-dibutyl ester (**4b**)

Aspect: orange oil. **yield:** 55%. **IR (NaCl):** 3437.0 (st, NH); 3101.4 (st, CH_{aromatic}); 2960.6, 2931.7 and 2879.6 (st_{ass}, CH₃ and CH₂); 1591.2 (st, C=N); 1471.6 (δ_{ass}, CH₂ and CH₃); 1394.4 (δ_{sim}, CH₃); 1240.1 (st P=O); 1110.9 (st P–N); 1029.9 (st P–O–C). **NMR ¹H (DMSO):** 9.96 [d, (P–N–H), J_{HP} = 28.10 Hz, 1H]; 8.57 [d, (H₂ and H₆), J_{ortho} = 6.21 Hz, 2H]; 7.88 [s, (N=C–H), 1H]; 7.48 [d, (H₃ and H₅), J_{ortho} = 6.21 Hz, 2H]; 3.83 [m, (CH₂OP), 4H]; 1.57 [qui, (CH₂CH₂OP), J_{HH} = 6.47 Hz, 4H]; 1.33 [sex, (CH₂(CH₂)₂OP), J_{HH} = 7.02 Hz, 4H]; 0.84 [t, (CH₃(CH₂)₃OP), J_{HH} = 7.55 Hz, 6H]. **NMR ¹³C (DMSO):** 150.13 [s, (C₂ and C₆), 2C]; 141.80 [s, (C₄), 1C]; 141.34 [d, (N=C), J_{CP} = 20.01 Hz, 1C]; 120.18 [s, (C₃ and C₅), 1C]; 66.04 [d, (CH₂OP), J_{CP} = 5.35 Hz, 2C]; 31.74 [d, (CH₂CH₂OP), J_{CP} = 6.57 Hz, 2C]; 18.18 [s, (CH₂CH₂CH₂OP), 2C]; 13.37 [s, (CH₃CH₂CH₂CH₂OP), 2C]. **NMR ³¹P (DMSO):** 1.33 [dq, (P–N–H), J_{HP} = 27.56 Hz, (CH₂OP), J_{HP} = 7.35 Hz]. Coupled. **m/z:** 41(13%), 80(4%), 98(100%), 124(4%), 154(22%), 202(2%), 214(<2%), 258(<2%), 270(<2%), 314(<2%). HR-MS (ESI) calc. for C₁₄H₂₄N₃O₃P (M)⁺: 313.155528, found: (M + H)⁺: 314.162805, (M + Na)⁺: 336.144749.

6.3. Phosphorohydrazidic acid, *N'*-[(1*E*)-4-pyridinylmethylene]-diisopropyl ester (**4c**)

Aspect: orange solid. **MP:** 156–158 °C. **yield:** 52%. **IR (NaCl):** 3431.2 (st, NH); 3116.8 (st, CH_{aromatic}); 2979.9, 2933.6 and 2823.6 (st_{ass.}, CH₃ and CH₂); 1597.0 (st, C=N); 1481.2 (δ_{ass.}, CH₂ and CH₃); 1386.7 (δ_{sim.}, CH₃); 1236.3 (st, P=O); 1114.8 (st, P–N); 1014.5 (st, P–O–C). **NMR ¹H (DMSO):** 9.87 [d, (P–NH), *J*_{HP} = 28.92 Hz, 1H]; 8.57 [d, (H₂ and H₆), *J*_{ortho} = 6.77 Hz, 2H]; 7.88 [s, (N=C–H), 1H]; 7.50 [d, (H₃ and H₅), *J*_{ortho} = 6.77 Hz, 2H]; 4.55 [m, (CHOP), 2H]; 1.27 [d, ((CH₃)₂CHOP), *J*_{HH} = 6.42 Hz, 6H]; 1.22 [d, ((CH₃)₂CHOP), *J*_{HH} = 6.42 Hz, 6H]. **NMR ¹³C (DMSO):** 149.80 [s, (C₂ and C₆), 2C]; 142.25 [s, (C₄), 1C]; 140.83 [d, (N=C), *J*_{CP} = 21.02 Hz, 1C]; 120.20 [s, (C₃ and C₅), 1C]; 71.00 [d, (CHOP), *J*_{CP} = 5.97 Hz, 2C]; 23.56 [d, ((CH₃)₂CHOP), *J*_{CP} = 4.41 Hz, 2C]. **NMR ³¹P (DMSO):** –0.79 [dt, (P–N–H), *J*_{HP} = 29.52 Hz, (CHOP), *J*_{HP} = 7.64 Hz]. coupled. **m/z:** 43(27%), 81(11%), 98(100%), 120(4%), 140(17%), 184(6%), 200(1%), 228(5%), 242(2%), 286(<2%). HR-MS (ESI) calc. for C₁₂H₂₀N₃O₃P (M)⁺: 285.124228, found: (M + H)⁺: 286.131504, (M + Na)⁺: 308.113449.

6.4. Phosphorohydrazidic acid, *N'*-[(1*E*)-4-pyridinylmethylene]-diisobutyl ester (**4d**)

Aspect: yellow solid. **MP:** 110–112 °C. **yield:** 43%. **IR (NaCl):** 3453.1 (st, NH); 3097.5 (st, CH_{aromatic}); 2956.7, 2925.9 and 2821.7 (st_{ass.}, CH₃ and CH₂); 1597.0 (st, C=N); 1475.5 (δ_{ass.}, CH₂ and CH₃); 1409.9 (δ_{sim.}, CH₃); 1245.9 (st, P=O); 1105.1 (st, P–N); 1033.8 (st, P–O–C). **NMR ¹H (DMSO):** 9.98 [d, (P–N–H), *J*_{HP} = 29.0 Hz, 1H]; 8.57 [d, (H₂ and H₆), *J*_{ortho} = 6.27 Hz, 2H]; 7.88 [s, (N=C–H), 1H]; 7.48 [d, (H₃ and H₅), *J*_{ortho} = 6.27 Hz, 2H]; 3.77 [m, (CH₂OP), 4H]; 1.88 [m, (CHCH₂OP), *J*_{HH} = 6.69 Hz, 2H]; 0.88 [d, ((CH₃)₂CHCH₂OP), *J*_{HH} = 6.97 Hz, 12H]. **NMR ¹³C (DMSO):** 150.10 [s, (C₂ and C₆), 2C]; 141.84 [s, (C₄), 1C]; 141.31 [d, (N=C), *J*_{CP} = 18.90 Hz, 1C]; 120.16 [s, (C₃ and C₅), 1C]; 72.26 [d, (CH₂OP), *J*_{CP} = 6.28 Hz, 2C]; 28.57 [d, (CHCH₂OP), *J*_{CP} = 6.76 Hz, 2C]; 18.51 [d, ((CH₃)₂CHCH₂OP), *J*_{CP} = 3.97 Hz, 4C]. **NMR ³¹P (DMSO):** 1.14 [dq, (P–N–H), *J*_{HP} = 29.0 Hz, (CH₂OP), *J*_{HP} = 8.00 Hz]. Coupled. **m/z:** 57(16%), 92(3%), 98(100%), 138(3%), 154(10%), 202(2%), 214(1%), 242(3%), 314(<1%). HR-MS (ESI) calc. for C₁₄H₂₄N₃O₃P (M)⁺: 313.155528, found: (M + H)⁺: 314.162805, (M + Na)⁺: 336.144749.

6.5. Phosphorohydrazidic acid, *N'*-[(1*E*)-3-pyridinylmethylene]-diethyl ester (**4e**)

Aspect: yellow oil. **yield:** 55%. **IR (NaCl):** 3427.3 (st, NH); 3165.0 (st, CH_{aromatic}); 2985.7 and 2927.8 (st_{ass.}, CH₃ and CH₂); 1604.7 (st, C=N); 1475.5 (δ_{ass.}, CH₂ and CH₃); 1413.7 (δ_{sim.}, CH₃); 1238.2 (st, P=O); 1163.0 (st, P–N); 1031.8 (st, P–O–C). **NMR ¹H (DMSO):** 9.77 [d, (P–N–H), *J*_{HP} = 28.48 Hz, 1H]; 8.69 [d, (H₂), *J*_{HH} = 1.71 Hz, 1H]; 8.52 [dd, (H₆), *J*_{ortho} = 4.83 Hz, *J*_{meta} = 1.71 Hz, 1H]; 7.94 [m, (N=CH and H₄), 2H]; 7.40 [dd, (H₅), *J*_{ortho} = 4.71 Hz and 7.90 Hz, 1H]; 4.04 [m, (CH₃CH₂OP), 4H]; 1.23 [t, (CH₃CH₂OP), *J*_{HH} = 6.90 Hz, 6H]. **NMR ¹³C (DMSO):** 149.82 [s, (C₆), 1C]; 147.77 [s, (C₂), 1C]; 141.01 [d, (N=C), *J*_{CP} = 19.02 Hz, 1C]; 132.65 [s, (C₄), 1C]; 130.53 [s, (C₃), 1C]; 123.89 [s, (C₅), 1C]; 62.45 [d, (CH₂OP), *J*_{CP} = 5.48 Hz, 2C]; 16.03 [d, (CH₃CH₂OP), *J*_{CP} = 5.48 Hz, 2C]. **NMR ³¹P (DMSO):** 1.61 [dq, (P–N–H), *J*_{HP} = 29.89 Hz, (CH₂OP), *J*_{HP} = 7.35 Hz]. Coupled. **m/z:** 51(5%), 65(38%), 92(96%), 120(100%), 133(2%), 155(2%), 184(2%), 200(<1%), 229(<1%), 257(8%). HR-MS (ESI) calc. for C₁₀H₁₆N₃O₃P (M)⁺: 257.092928, found: (M + H)⁺: 258.100204, (M + Na)⁺: 280.082149.

6.6. Phosphorohydrazidic acid, *N'*-[(1*E*)-3-pyridinylmethylene]-dibutyl ester (**4f**)

Aspect: orange oil. **yield:** 55%. **IR (NaCl):** 3431.2 (st, NH); 3101.4 (st, CH_{aromatic}); 2960.6, 2931.7 and 2873.8 (st_{ass.}, CH₃ and CH₂); 1600.8 (st, C=N); 1465.8 (δ_{ass.}, CH₂ and CH₃); 1419.5 (δ_{sim.}, CH₃); 1242.1 (st, P=O); 1066.6 (st, P–N); 1029.9 (st, P–O–C). **NMR ¹H (DMSO):** 9.77 [d, (P–N–H), *J*_{HP} = 28.02 Hz, 1H]; 8.70 [d, (H₂), *J*_{HH} = 1.70 Hz, 1H]; 8.52 [dd, (H₆), *J*_{ortho} = 4.74 Hz and 1.58 Hz, 1H]; 7.93 [s, (N=CH), 1H]; 7.92 [td (H₄), *J*_{ortho} = 6.45 Hz, *J*_{meta} = 1.94 Hz, 1H]; 7.41 [dd, (H₅), *J*_{ortho} = 4.61 Hz and 7.83 Hz, 1H]; 3.98 [m, (CH₂OP), 4H]; 1.57 [m, (CH₂CH₂OP), 4H]; 1.33 [sex, (CH₂(CH₂)₂OP), *J*_{HH} = 7.39 Hz, 4H]; 0.84 [t, (CH₃(CH₂)₃OP), *J*_{HH} = 7.20 Hz, 6H]. **NMR ¹³C (DMSO):** 149.83 [s, (C₆), 1C]; 147.72 [s, (C₂), 1C]; 140.90 [d, (N=C), *J*_{CP} = 20.84 Hz, 1C]; 132.63 [s, (C₄), 1C]; 130.56 [s, (C₃), 1C]; 123.90 [s, (C₅), 1C]; 65.95 [d, (CH₂OP), *J*_{CP} = 6.64 Hz, 2C]; 31.71 [d, (CH₂CH₂OP), *J*_{CP} = 6.64 Hz, 2C]; 18.20 [s, (CH₂CH₂CH₂OP), 2C]; 13.38 [s, (CH₃CH₂CH₂CH₂OP), 2C]. **NMR ³¹P (DMSO):** 1.73 [dq, (P–N–H), *J*_{HP} = 27.47 Hz, (CH₂OP), *J*_{HP} = 7.84 Hz]. coupled. **m/z:** 41(11%), 80(5%), 98(100%), 124(7%), 154(21%), 184(2%), 214(1%), 258(1%), 270(<1%), 314(1%). HR-MS (ESI) calc. for C₁₄H₂₄N₃O₃P (M)⁺: 313.155528, found: (M + H)⁺: 314.162805, (M + Na)⁺: 336.144749.

6.7. Phosphorohydrazidic acid, *N'*-[(1*E*)-3-pyridinylmethylene]-diisopropyl ester (**4g**)

Aspect: orange oil. **yield:** 55%. **IR (NaCl):** 3431.2 (st, NH); 3099.5 (st, CH_{aromatic}); 2979.9, 2925.9 and 2817.9 (st_{ass.}, CH₃ and CH₂); 1604.7 (st, C=N); 1475.5 (δ_{ass.}, CH₂ and CH₃); 1380.9 (δ_{sim.}, CH₃); 1245.9 (st, P=O); 1097.4 (st, P–N); 1028.0 (st, P–O–C). **NMR ¹H (DMSO):** 9.67 [d, (P–N–H), *J*_{HP} = 28.32 Hz, 1H]; 8.70 [d, (H₂), *J*_{HH} = 1.75 Hz, 1H]; 8.52 [dd, (H₆), *J*_{ortho} = 4.92 Hz and 1.66 Hz, 1H]; 7.94 [m, (N=CH) and (H₄), 2H]; 7.41 [dd, (H₅), *J*_{ortho} = 4.72 Hz and 7.94 Hz, 1H]; 4.54 [m, (CHOP), 2H]; 1.23 [d, (CH₃)₂CHOP), *J*_{HH} = 6.22 Hz, 6H]; 1.19 [d, (CH₃)₂CHOP), *J*_{HH} = 6.22 Hz, 6H]. **NMR ¹³C (DMSO):** 149.57 [s, (C₆), 1C]; 147.51 [s, (C₂), 1C]; 140.43 [d, (N=C), *J*_{CP} = 19.15 Hz, 1C]; 132.63 [s, (C₄), 1C]; 130.71 [s, (C₃), 1C]; 123.93 [s, (C₅), 1C]; 70.82 [d, (CHOP), *J*_{CP} = 5.32 Hz, 2C]; 23.58 [d, (CH₃)₂CHOP), *J*_{CP} = 4.52 Hz, 2C]; 23.34 [d, (CH₃)₂CHOP), *J*_{CP} = 4.52 Hz, 2C]. **NMR ³¹P (DMSO):** –0.15 [dt, (P–N–H), *J*_{HP} = 27.54 Hz, (CHOP), *J*_{HP} = 7.36 Hz]. coupled. **m/z:** 43(22%), 81(11%), 98(100%), 120(19%), 140(16%), 184(6%), 200(1%), 228(3%), 242(1%), 285(1%). HR-MS (ESI) calc. for C₁₂H₂₀N₃O₃P (M)⁺: 285.124228, found: (M + H)⁺: 286.131504, (M + Na)⁺: 308.113449.

6.8. Phosphorohydrazidic acid, *N'*-[(1*E*)-3-pyridinylmethylene]-diisobutyl ester (**4h**)

Aspect: white solid. **MP:** 92–94 °C. **yield:** 47%. **IR (NaCl):** 3435.1 (st, NH); 3097.5 (st, CH_{aromatic}); 2956.7, 2927.8 and 2823.6 (st_{ass.}, CH₃ and CH₂); 1606.6 (st, C=N); 1465.8 (δ_{ass.}, CH₂ and CH₃); 1398.3 (δ_{sim.}, CH₃); 1247.9 (st, P=O); 1093.6 (st, P–N); 1031.8 (st, P–O–C). **NMR ¹H (DMSO):** 9.78 [d, (P–N–H), *J*_{HP} = 28.52 Hz, 1H]; 8.70 [d, (H₂), *J*_{HH} = 1.86 Hz, 1H]; 8.52 [dd, (H₆), *J*_{ortho} = 4.76 Hz and 1.65 Hz, 1H]; 7.93 [s, (N=CH), 1H]; 7.92 [td (H₄), *J*_{ortho} = 7.04 Hz, *J*_{meta} = 1.86 Hz, 1H]; 7.42 [dd, (H₅), *J*_{ortho} = 4.26 Hz and 7.65 Hz, 1H]; 3.77 [m, (CH₂OP), 4H]; 1.88 [m, (CHCH₂OP), *J*_{HH} = 6.50 Hz, 2H]; 0.88 [d, ((CH₃)₂CHCH₂OP), *J*_{HH} = 7.66 Hz, 12H]. **NMR ¹³C (DMSO):** 149.76 [s, (C₆), 1C]; 147.64 [s, (C₂), 1C]; 140.84 [d, (N=C), *J*_{CP} = 19.30 Hz, 1C]; 132.61 [s, (C₄), 1C]; 130.58 [s, (C₃), 1C]; 123.91 [s, (C₅), 1C]; 72.12 [d, (CH₂OP), *J*_{CP} = 6.37 Hz, 2C]; 28.57 [d, (CHCH₂OP), *J*_{CP} = 6.37 Hz, 2C]; 18.53 [d, (CH₃)₂CHCH₂OP), *J*_{CP} = 3.70 Hz, 4C]. **NMR ³¹P (DMSO):** 1.64 [dq, (P–N–H), *J*_{HP} = 30.5 Hz, (CH₂OP), *J*_{HP} = 7.56 Hz]. coupled. **m/z:** 57(13%), 92(4%), 98(100%), 138(4%),

154(11%), 184(3%), 214(1%), 242(1%), 313(<1%). HR-MS (ESI) calc. for $C_{14}H_{24}N_3O_3P$ (M)⁺: 313.155528, found: ($M + H$)⁺: 314.162805, ($M + Na$)⁺: 336.144749.

6.9. Phosphorohydrazidic acid, *N'*-[(1*E,Z*)-2-pyridinylmethylene]-diethyl ester (**4i**)

Aspect: dark oil. **yield:** 36%. **IR (NaCl):** 3433.1 (st, NH); 3140.0 (st, $CH_{aromatic}$); 2983.7, 2931.7 and 2912.4 ($st_{ass.}, CH_3$ and CH_2); 1585.4 (st, $C=N$); 1461.9 ($\delta_{ass.}, CH_2$ and CH_3); 1394.4 ($\delta_{sim.}, CH_3$); 1240.1 (st, $P=O$); 1164.9 (st, $P-N$); 1028.0 (st, $P-O-C$). **NMR ¹H (DMSO):** 9.84 [d, ($P-N-H$), $J_{HP} = 27.94$ Hz, 1H]; 8.53 [ddd, (H_6), $J_{ortho} = 4.93$ Hz, $J_{meta} = 1.82$ Hz, $J_{para} = 0.64$ Hz, 1H]; 7.96 [s, ($N=CH$), 1H]; 7.79 [dt, (H_4), $J_{ortho} = 7.64$ Hz, $J_{meta} = 1.96$ Hz, 1H]; 7.75 [td, (H_3), $J_{ortho} = 7.82$ Hz, $J_{meta} = 1.10$ Hz, 1H]; 7.33 [ddd, (H_3), $J_{ortho} = 7.52$ Hz, $J_{ortho} = 5.37$ Hz, $J_{meta} = 1.28$ Hz, 1H]; 4.03 [m, (CH_2OP), 4H]; 1.24 [t, (CH_3CH_2OP), $J_{HH} = 7.23$ Hz, 6H]. **NMR ¹³C (DMSO):** 153.49 [s, (C_2), 1C]; 149.30 [s, (C_5), 1C]; 144.60 [d, ($N=C$), $J_{CP} = 19.15$ Hz, 1C]; 136.74 [s, (C_6), 1C]; 123.66 [s, (C_4), 1C]; 119.03 [s, (C_3), 1C]; 62.56 [d, (CH_2OP), $J_{CP} = 5.67$ Hz, 2C]; 16.04 [d, (CH_3CH_2OP), $J_{CP} = 6.60$ Hz, 2C]. **NMR ³¹P (DMSO):** 1.53 [dq, ($P-N-H$), $J_{HP} = 28.25$ Hz, (CH_2OP), $J_{HP} = 7.70$ Hz]; 0.97 [td, ($P-N-H$), $J_{HP} = 34.01$ Hz, (CH_2OP), $J_{HP} = 7.70$ Hz]. Coupled. **m/z:** 51(5%), 65(39%), 92(94%), 120(100%), 133(2%), 155(2%), 184(2%), 200(<1%), 229(<1%), 257(7%). HR-MS (ESI) calc. for $C_{10}H_{16}N_3O_3P$ (M)⁺: 257.092928, found: ($M + H$)⁺: 258.100204, ($M + Na$)⁺: 280.082149.

6.10. Phosphorohydrazidic acid, *N'*-[(1*E,Z*)-2-pyridinylmethylene]-dibutyl ester (**4j**)

Aspect: dark oil. **yield:** 45%. **IR (NaCl):** 3429.3 (st, NH); 3136.1 (st, $CH_{aromatic}$); 2960.6 and 2877.7 ($st_{ass.}, CH_3$ and CH_2); 1585.4 (st, $C=N$); 1463.9 ($\delta_{ass.}, CH_2$ and CH_3); 1386.7 ($\delta_{sim.}, CH_3$); 1240.1 (st, $P=O$); 1110.9 (st, $P-N$); 1028.0 (st, $P-O-C$). **NMR ¹H (DMSO):** 9.85 [d, ($P-N-H$), $J_{HP} = 28.72$ Hz, 1H]; 8.53 [ddd, (H_6), $J_{ortho} = 5.04$ Hz, $J_{meta} = 1.84$ Hz, $J_{para} = 0.96$ Hz, 1H]; 7.95 [s, ($N=CH$), 1H]; 7.79 [dt, (H_4), $J_{ortho} = 7.73$ Hz, $J_{meta} = 1.89$ Hz, 1H]; 7.74 [td, (H_3), $J_{ortho} = 7.87$ Hz, $J_{meta} = 1.10$ Hz, 1H]; 7.34 [ddd, (H_3), $J_{ortho} = 7.37$ Hz, $J_{ortho} = 5.28$ Hz, $J_{meta} = 1.32$ Hz, 1H]; 3.98 [m, (CH_2OP), 4H]; 1.57 [m, (CH_2CH_2OP), 4H]; 1.34 [sex, ($CH_2(CH_2)_2OP$), $J_{HH} = 7.28$ Hz, 4H]; 0.84 [t, ($CH_3(CH_2)_3OP$), $J_{HH} = 7.25$ Hz, 6H]. **NMR ¹³C (DMSO):** 153.54 [s, (C_2), 1C]; 149.29 [s, (C_5), 1C]; 144.49 [d, ($N=C$), $J_{CP} = 19.11$ Hz, 1C]; 136.68 [s, (C_6), 1C]; 123.63 [s, (C_4), 1C]; 118.85 [s, (C_3), 1C]; 65.98 [d, (CH_2OP), $J_{CP} = 5.49$ Hz, 2C]; 31.76 [d, (CH_2CH_2OP), $J_{CP} = 6.34$ Hz, 2C]; 18.19 [s, ($CH_2CH_2CH_2OP$), 2C]; 13.36 [s, ($CH_3CH_2CH_2CH_2OP$), 2C]. **NMR ³¹P (DMSO):** 1.54 [dq, ($P-N-H$), $J_{HP} = 29.41$ Hz, (CH_2OP), $J_{HP} = 7.66$ Hz]; 1.05 [td, ($P-N-H$), $J_{HP} = 34.83$ Hz, (CH_2OP), $J_{HP} = 7.66$ Hz]. Coupled. **m/z:** 65(19%), 92(67%), 120(100%), 133(2%), 161(4%), 184(1%), 208(2%), 258(1%), 270(<1%), 313(1%). HR-MS (ESI) calc. for $C_{14}H_{24}N_3O_3P$ (M)⁺: 313.155528, found: ($M + H$)⁺: 314.162805, ($M + Na$)⁺: 336.144749.

6.11. Phosphorohydrazidic acid, *N'*-[(1*E*)-2-pyridinylmethylene]-diisopropyl ester (**4k**)

Aspect: white solid. **MP:** 171–173 °C. **yield:** 54%. **IR (NaCl):** 3427.3 (st, NH); 3136.1 (st, $CH_{aromatic}$); 2981.8, 2943.2 and 2839.1 ($st_{ass.}, CH_3$ and CH_2); 1583.5 (st, $C=N$); 1456.2 ($\delta_{ass.}, CH_2$ and CH_3); 1382.9 ($\delta_{sim.}, CH_3$); 1228.6 (st, $P=O$); 1110.9 (st, $P-N$); 1024.1 (st, $P-O-C$). **NMR ¹H (DMSO):** 9.74 [d, ($P-N-H$), $J_{HP} = 27.83$ Hz, 1H]; 8.53 [ddd, (H_6), $J_{ortho} = 5.24$ Hz, $J_{meta} = 1.95$ Hz, $J_{para} = 0.86$ Hz, 1H]; 7.96 [s, ($N=CH$), 1H]; 7.79 [dt, (H_4), $J_{ortho} = 7.91$ Hz, $J_{meta} = 1.88$ Hz, 1H]; 7.74 [td, (H_3), $J_{ortho} = 7.65$ Hz, $J_{meta} = 1.25$ Hz, 1H]; 7.32 [ddd, (H_5), $J_{ortho} = 7.45$ Hz, $J_{ortho} = 5.43$ Hz, $J_{meta} = 1.51$ Hz, 1H]; 4.55 [m, ($CHOP$), 2H]; 1.34 [d, (CH_3)₂CHOP], $J_{HH} = 6.35$ Hz, 6H];

1.28 [d, (CH_3)₂CHOP], $J_{HH} = 6.35$ Hz, 6H]. **NMR ¹³C (DMSO):** 153.64 [s, (C_2), 1C]; 149.25 [s, (C_5), 1C]; 144.12 [d, ($N=C$), $J_{CP} = 18.42$ Hz, 1C]; 136.71 [s, (C_6), 1C]; 123.52 [s, (C_4), 1C]; 118.77 [s, (C_3), 1C]; 70.90 [d, ($CHOP$), $J_{CP} = 5.51$ Hz, 2C]; 23.55 [d, (CH_3)₂CHOP], $J_{CP} = 4.82$ Hz, 2C]; 23.34 [d, (CH_3)₂CHOP], $J_{CP} = 4.82$ Hz, 2C]. **NMR ³¹P (DMSO):** -0.36 [dt, ($P-N-H$), $J_{HP} = 27.43$ Hz, ($CHOP$), $J_{HP} = 7.34$ Hz]. Coupled. **m/z:** 43(16%), 65(20%), 92(56%), 120(100%), 147(5%), 184(5%), 201(1%), 228(2%), 243(23%), 285(5%). HR-MS (ESI) calc. for $C_{12}H_{20}N_3O_3P$ (M)⁺: 285.124228, found: ($M + H$)⁺: 286.131504, ($M + Na$)⁺: 308.113449.

6.12. Phosphorohydrazidic acid, *N'*-[(1*E*)-2-pyridinylmethylene]-diisobutyl ester (**4l**)

Aspect: brown solid. **MP:** 90–92 °C. **yield:** 50%. **IR (NaCl):** 3438.9 (st, NH); 3134.2 (st, $CH_{aromatic}$); 2958.7, 2875.7 ($st_{ass.}, CH_3$ and CH_2); 1585.4 (st, $C=N$); 1461.9 ($\delta_{ass.}, CH_2$ and CH_3); 1371.3 ($\delta_{sim.}, CH_3$); 1228.6 (st, $P=O$); 1103.2 (st, $P-N$); 1018.3 (st, $P-O-C$). **NMR ¹H (DMSO):** 9.84 [d, ($P-N-H$), $J_{HP} = 28.90$ Hz, 1H]; 8.52 [ddd, (H_6), $J_{ortho} = 4.82$ Hz, $J_{meta} = 1.92$ Hz, $J_{para} = 0.63$ Hz, 1H]; 7.95 [s, ($N=CH$), 1H]; 7.80 [dt, (H_4), $J_{ortho} = 7.75$ Hz, $J_{meta} = 1.64$ Hz, 1H]; 7.72 [td, (H_3), $J_{ortho} = 7.90$ Hz, $J_{meta} = 1.16$ Hz, 1H]; 7.32 [ddd, (H_5), $J_{ortho} = 7.51$ Hz, $J_{ortho} = 6.11$ Hz, $J_{meta} = 1.36$ Hz, 1H]; 3.78 [m, (CH_2OP), 4H]; 1.88 [n, $CHCH_2OP$], $J_{HH} = 6.61$ Hz, 2H]; 0.87 [d, (CH_3)₂CHCH₂OP], $J_{HH} = 6.98$ Hz, 12H]. **NMR ¹³C (DMSO):** 153.54 [s, (C_2), 1C]; 149.28 [s, (C_5), 1C]; 144.46 [d, ($N=C$), $J_{CP} = 19.80$ Hz, 1C]; 136.71 [s, (C_6), 1C]; 123.61 [s, (C_4), 1C]; 118.76 [s, (C_3), 1C]; 72.15 [d, (CH_2OP), $J_{CP} = 6.51$ Hz, 2C]; 28.51 [d, ($CHCH_2OP$), $J_{CP} = 6.25$ Hz, 2C]; 18.50 [d, (CH_3)₂CHCH₂OP], $J_{CP} = 3.50$ Hz, 4C]. **NMR ³¹P (DMSO):** 1.43 [dq, ($P-N-H$), $J_{HP} = 30.05$ Hz, (CH_2OP), $J_{HP} = 7.12$ Hz]. Coupled. **m/z:** 65(17%), 92(61%), 120(100%), 123(1%), 161(5%), 202(4%), 214(<1%), 258(4%), 313(2%). HR-MS (ESI) calc. for $C_{14}H_{24}N_3O_3P$ (M)⁺: 313.155528, found: ($M + H$)⁺: 314.162805, ($M + Na$)⁺: 336.144749.

6.13. Phosphorohydrazidic acid, *N'*-[(1*E*)-(5-bromo-3-pyridinyl)methylene]-disecbutyl ester (**4m**)

Aspect: white solid. **MP:** 121–122 °C. **yield:** 62%. **IR (NaCl):** 3440.9 (st, NH); 3101.4 (st, $CH_{aromatic}$); 2972.2, 2931.7 and 2827.5 ($st_{ass.}, CH_3$ and CH_2); 1600.8 (st, $C=N$); 1471.6 ($\delta_{ass.}, CH_2$ and CH_3); 1242.1 (st, $P=O$); 1095.5 (st, $P-N$); 1018.3 (st, $P-O-C$). **NMR ¹H (DMSO):** 9.91 [d, ($P-N-H$), $J_{HP} = 28.62$ Hz, 1H]; 8.70 [s, (H_6), 1H]; 8.64 [s, (H_2), 1H]; 8.12 [s, ($N=CH$), 1H]; 7.89 [s, (H_4), 1H]; 4.34 [m, ($CHOP$), 2H]; 1.55 [m, (CH_2CHOP), 4H]; 1.27 [d, (CH_3CHOP), $J_{HH} = 5.45$ Hz, 3H]; 1.21 [d, (CH_3CHOP), $J_{HH} = 5.45$ Hz, 3H]; 0.88 [t, (CH_3CH_2CHOP), $J_{HH} = 7.80$ Hz, 3H]; 0.84 [t, (CH_3CH_2CHOP), $J_{HH} = 7.80$ Hz, 3H]. **NMR ¹³C (DMSO):** 150.00 [s, (C_6), 1C]; 145.90 [s, (C_2), 1C]; 138.68 [d, ($N=C$), $J_{CP} = 19.85$ Hz, 1C]; 134.62 [s, (C_4), 1C]; 132.70 [s, (C_3), 1C]; 120.48 [s, (C_5), 1C]; 75.55 [t, ($CHOP$), $J_{CP} = 5.76$ Hz, 2C]; 29.84 [d, (CH_2CHOP), $J_{CP} = 6.00$ Hz, 1C]; 29.68 [d, (CH_2CHOP), $J_{CP} = 6.00$ Hz, 1C]; 21.10 [d, (CH_3CHOP), $J_{CP} = 2.63$ Hz, 1C]; 20.82 [d, (CH_3CHOP), $J_{CP} = 2.63$ Hz, 1C]; 9.32 [d, (CH_3CH_2CHOP), $J_{CP} = 6.72$ Hz, 2C]. **NMR ³¹P (DMSO):** -0.30 [dt, ($P-N-H$), $J_{HP} = 27.97$ Hz, (CH_2OP), $J_{HP} = 8.13$ Hz]; Coupled. **m/z:** 57(17%), 91(4%), 98(100%), 137(1%), 154(5%), 200(5%), 262(4%), 280(1%), 306(2%), 392(<1%). HR-MS (ESI) calc. for $C_{14}H_{23}BrN_3O_3P$ (M)⁺: 391.066041, found: ($M + H$)⁺: 392.073317, ($M + Na$)⁺: 414.055262.

6.14. Phosphorohydrazidic acid, *N'*-[(1*E*)-(2-bromo-3-pyridinyl)methylene]-disecbutyl ester (**4n**)

Aspect: yellow oil. **yield:** 64%. **IR (NaCl):** 3435.1 (st, NH); 3134.2 (st, $CH_{aromatic}$); 2974.1, 2937.5 and 2879.6 ($st_{ass.}, CH_3$ and CH_2);

1577.7 (st, C=N); 1460.0 ($\delta_{\text{ass.}}$, CH₂ and CH₃); 1392.6 ($\delta_{\text{sym.}}$, CH₃); 1234.4 (st, P=O); 1105.2 (st, P–N); 1002.9 (st, P–O–C). **NMR** ¹H (DMSO): 10.00 [d, (P–N–H), $J_{\text{HP}} = 29.20$ Hz, 1H]; 8.35 [dd, (H₆), $J_{\text{m}} = 2.12$ Hz, $J_{\text{o}} = 4.87$ Hz, 1H]; 8.17 [s, (N=CH), 1H]; 8.06 [dd, (H₄), $J_{\text{m}} = 1.94$ Hz, $J_{\text{o}} = 7.77$ Hz, 1H]; 7.50 [m, (H₅), 1H]; 4.35 [m, (CHOP), 2H]; 1.55 [m, (CH₂CHOP), 2H]; 1.25 [d, (CH₃CHOP), $J_{\text{HH}} = 6.08$ Hz, 3H]; 1.20 [d, (CH₃CHOP), $J_{\text{HH}} = 6.08$ Hz, 3H]; 0.87 [t, (CH₃CH₂CHOP), $J_{\text{HH}} = 7.44$ Hz, 3H]; 0.84 [t, (CH₃CH₂CHOP), $J_{\text{HH}} = 7.44$ Hz, 3H]. **NMR** ¹³C (DMSO): 150.36 [s, (C₆), 1C]; 141.21 [s, (C₂), 1C]; 140.02 [d, (N=C), $J_{\text{CP}} = 18.22$ Hz, 1C]; 134.53 [s, (C₄), 1C]; 131.10 [s, (C₃), 1C]; 123.96 [s, (C₅), 1C]; 75.66 [m, (CHOP), 2C]; 29.84 [d, (CH₂CHOP), $J_{\text{CP}} = 4.19$ Hz, 1C]; 29.73 [d, (CH₂CHOP), $J_{\text{CP}} = 4.19$ Hz, 1C]; 21.10 [d, (CH₃CHOP), $J_{\text{CP}} = 3.60$ Hz, 1C]; 20.83 [d, (CH₃CHOP), $J_{\text{CP}} = 3.60$ Hz, 1C]; 9.38 [d, (CH₃CH₂CHOP), $J_{\text{CP}} = 6.47$ Hz, 2C]. **NMR** ³¹P (DMSO): –0.46 [dt, (P–N–H), $J_{\text{HP}} = 29.45$ Hz, (CHOP), $J_{\text{HP}} = 8.12$ Hz]; coupled. **m/z**: 41(28%), 57(20%), 73(10%), 98(100%), 103(6%), 120(7%), 154(4%), 185(5%), (392(<1%)). HR-MS (ESI) calc. for C₁₄H₂₃BrN₃O₃P (M)⁺: 391.066041, found: (M + H)⁺: 392.073317, (M + Na)⁺: 414.055262.

6.15. Phosphorohydrazidic acid, N'-[(1E)-(3,5-dichloro-4-pyridinyl)methylene]-disecbutyl ester (40)

Aspect: yellow oil. **yield:** 64%. **IR (NaCl):** 3423.5 (st, NH); 3128.4 (st, CH_{aromatic}); 2974.1 and 2929.7 (st_{ass.}, CH₃ and CH₂); 1600.8 (st, C=N); 1465.2 ($\delta_{\text{ass.}}$, CH₂ and CH₃); 1388.7 ($\delta_{\text{sym.}}$, CH₃); 1238.2 (st, P=O); 1109.3 (st, P–N); 1004.8 (st, P–O–C). **NMR** ¹H (DMSO): 10.16 [d, (P–N–H), $J_{\text{HP}} = 29.74$ Hz, 1H]; 8.63 [s, (H₂ and H₆), 2H]; 8.13 [s, (N=CH), 1H]; 4.36 [m, (CHOP), 2H]; 1.56 [m, (CH₂CHOP), 4H]; 1.24 [d, (CH₃CHOP), $J_{\text{HH}} = 6.07$ Hz, 3H]; 1.20 [d, (CH₃CHOP), $J_{\text{HH}} = 6.07$ Hz, 3H]; 0.86 [t, (CH₃CH₂CHOP), $J_{\text{HH}} = 7.29$ Hz, 3H]; 0.83 [t, (CH₃CH₂CHOP), $J_{\text{HH}} = 7.29$ Hz, 3H]. **NMR** ¹³C (DMSO): 148.87 [s, (C₂ and C₆), 2C]; 137.64 [d, (N=C), $J_{\text{CP}} = 20.19$ Hz, 1C]; 136.80 [s, (C₃ and C₅), 2C]; 130.33 [s, (C₄), 1C]; 76.17 [m, (CHOP), 2C]; 30.30 [d, (CH₂CHOP), $J_{\text{CP}} = 5.62$ Hz, 1C]; 30.14 [d, (CH₂CHOP), $J_{\text{CP}} = 5.62$ Hz, 1C]; 21.41 [d, (CH₃CHOP), $J_{\text{CP}} = 3.00$ Hz, 1C]; 21.30 [d, (CH₃CHOP), $J_{\text{CP}} = 3.00$ Hz, 1C]; 9.70 [s, (CH₃CH₂CHOP), 2C]. **NMR** ³¹P (DMSO): –1.54 [dt, (P–N–H), $J_{\text{HP}} = 29.97$ Hz, (CHOP), $J_{\text{HP}} = 8.12$ Hz]; Coupled. **m/z**: 57(15%), 98(100%), 124(2%), 154(5%), 252(2%), 296(2%), 326(<1%), 352(<1%), 382(<1%). HR-MS (ESI) calc. for C₁₄H₂₂Cl₂N₃O₃P (M)⁺: 381.077584, found: (M + H)⁺: 382.084860, (M + Na)⁺: 404.066805.

7. Biological evaluation

7.1. Macrophage culture

The J774 cell line-derived murine macrophage cells were provided by the Rio de Janeiro Cell Bank-HUCFF-UFRJ. The cells were grown in DMEM medium containing L-glutamine (2 mM), buffered with HEPES (10 mM), and supplemented with 10% heat-inactivated fetal calf serum and gentamicin (1 mg/L) in a humidified incubator (5% CO₂) at 37 °C. The cells were passaged twice per week.

7.2. Cytotoxicity assay in macrophages

J774 macrophages were seeded (1.5 × 10⁵ cells/well) in 96-well flat-bottom microplates with 100 μL of medium. The cells were allowed to attach to the bottom of the well for 24 h at 37 °C and then exposed to the different concentrations of compounds (100, 10 and 1 μM) for 48 h. Afterwards, the cells were washed with PBS and incubated with 3-(4,5-dimethylthiazol-2-yl)-2,5-diphenyltetrazolium bromide (MTT) (100 μL/well) for 1 h in the dark at 37 °C. The MTT solution was removed, the cells were resuspended in 100 μL of dimethylsulfoxide (DMSO), and the

absorbance was measured using an ELISA reader at 540 nm [22]. Each concentration was assayed in triplicate, and the corresponding cell growth controls were used in each measurement. The trials were also performed in duplicate.

7.3. Parasite culture

L. amazonensis [MHOM/BR/87/BA125] and *L. braziliensis* [MHOM/BR/01/BA788] strains were kindly provided by Valéria Borges, PhD (Fundação Oswaldo Cruz – BA/Brazil) and were maintained in vitro as proliferating promastigotes at 26 °C in Schneider's insect medium supplemented with 10% heat-inactivated fetal calf serum, gentamycin (1 mg/L), L-glutamine (2 mM) and 2% sterile human urine.

7.4. Leishmanicidal activity

Leishmania parasites were harvested at a late exponential phase of growth, resuspended in fresh medium, counted in a Neubauer's chamber and adjusted to a concentration of 10⁵ parasites/well in the presence of the corresponding concentration of compounds in a 96-microwell plate. They were allowed to proliferate in the presence of the compounds at 26 °C for 48 h for promastigotes. Then, the parasites were counted using an automatic cell counter [34]. All of the assays were performed in triplicate, and the experiments were repeated at least twice. The inhibition caused by each compound was expressed as a percentage relative to the control cells (treated with the vehicle, DMSO). The LD₅₀ and their standard errors were calculated using GraphPad Prism 5.0 software.

7.5. Antiamastigote assay

In vitro model of the amastigotes, inflammatory macrophages were obtained from BALB/c mice previously inoculated by the intraperitoneal route with 3% thyoglicollate medium (Sigma). Briefly, peritoneal macrophages were plated at 4 × 10⁵ cell/well on coverslips (Ø 13 cm) previously arranged in a 24-well plate in DMEM medium supplemented with 10% (v/v) heat-inactivated FBS and allowed to adhere overnight. Adherent macrophages were infected with *L. amazonensis* promastigote using a ratio of 1:10 at 37 °C for 4 h. Non-internalized promastigotes were eliminated, and solutions of tested compounds were added in different concentrations and maintained at 37 °C in 5% CO₂ for 48 h. Slides were fixed with methanol, stained with Giemsa and intracellular amastigotes were counted (two hundred macrophages were evaluated per assay). The results were analyzed using GraphPad Prism 5.0 software and expressed as infection index (percentage of infected macrophages multiplied by the average number of amastigotes per macrophage). Miltefosine was used as reference drug.

7.6. In vivo infection in a murine model

Female BALB/c mice, 6–8 weeks old, were obtained from the Federal University of Ribeirão Preto, Brazil. The animals were maintained under a 12-h light/dark cycle in a controlled-temperature room (22 ± 2 °C) with free access to water and pellet food. All of the procedures were performed after the approval of the protocol by the Ethics Committee - UFAL for animal handling (No: 2013.02).

A murine model closely resembling human pathology was previously described [23]. Briefly, the right ear dermis of BALB/c mice was inoculated with stationary-phase promastigotes of *L. amazonensis* (MHOM/BR/87/BA125), with 10⁵ parasites in 10 μL of sterile saline, using a 27.5-gauge needle. After the second week post-infection, a group of mice (n = 5) was treated daily (28 days) with

4m, **4n** or miltefosine (positive control) by oral administration at 30 mg/kg/day, diluted in water for administration. A negative control group was treated orally with water by injection ($n = 5$). Lesion size, which was defined as the difference in thickness (in millimeters) between the infected ear and the non-infected contralateral ear, was monitored twice weekly using a digital caliper.

7.7. Parasite load quantification

Parasite load was determined using a quantitative limiting dilution assay as previously described [35]. Briefly, infected ears and draining lymph nodes were aseptically excised after treatment and homogenized in Schneider medium. The homogenates were serially diluted in Schneider medium with 10% FCS and seeded into 96-well plates.

The data are reported as the average \pm standard error of the mean ($M \pm$ S.E.M) after statistical analysis employing one-way ANOVA followed by Dunnett's test. Differences between means were considered significant when $p < 0.05$ when compared to the control group. Calculations were performed using GraphPad 5.0 software.

7.8. Molecular modeling

According to the reasons presented above, we chose FPPS and the enzymes of the glycolytic and pentose phosphate pathways as possible targets in the molecular docking study. Glycolysis is a process catalyzed by ten enzymes: hexokinase (HK), glucose-6-phosphate isomerase (G6PI), phosphofructokinase (PFK), fructose biphosphate aldolase (FBPA), triose phosphate isomerase (TPI), glyceraldehyde-3-phosphate dehydrogenase (GPDH), phosphoglycerate kinase (PGK), phosphoglycerate mutase (PGM), enolase (ENO) and pyruvate kinase (PYK). The PPP is subdivided into two branches – the oxidative branch, comprising the enzymes glucose-6-phosphate dehydrogenase (G6PDH), 6-phosphogluconolactonase (6PGL) and 6-phosphogluconate dehydrogenase (6PGDH); and the non-oxidative branch, comprising the enzymes ribose-5-phosphate isomerase (RPI), ribulose-5-phosphate 4-epimerase (RPE), transaldolase (TAL) and transketolase (TKT).

In this group of enzymes, there is only one with an available crystallographic structure for one of the *Leishmania* species evaluated in the experimental section, namely, *L. braziliensis* 6PGL, which is deposited in the RCSB Protein Data Bank (PDB code 3CH7) with a resolution of 2.29 Å. For this structure, incomplete side chains were corrected using Swiss PDBViewer v. 4.1 [36], and water molecules were removed before the docking procedure. For the remaining *L. braziliensis* enzymes, sequences available in the UniProtKB/Swiss-Prot protein sequence database were used for construction of homology models using the automated mode of the Swiss-Model protein structure homology-modeling server [37]: A4HCH8 for FPPS, A4HBM3 for HK, A4H6W2 for PGI, A4HHQ0 for PFK, A4HNY6 for FBPA, E9AIG9 for TPI, A4HIN0 for GPDH, A4HIS6 for PGK, A4HLS3 for PGM, A4HL13 for ENO, A4HM36 for PYK, B0FGJ4 for 6PGDH, A7UFH5 for G6PDH, A4HGQ2 for RPI, A4HLL7 for RPE, A4H8J8 for TAL, and A4HDR8 for TKT. Unfortunately, there is a paucity of available crystallographic and sequence information for *L. amazonensis* enzymes, and it was only possible to find sequence data for two enzymes: Q8I911 for G6PDH, and B0FZP5 for 6PGDH, for which we constructed homology models according to the same procedure used for the *L. braziliensis* enzymes.

All of the ligand structures were constructed and energy-minimized with the PM3 method [38] available in the Spartan'14 software (Wavefunction, Inc.). The molecular docking study was carried out with GOLD 5.2 (CCDC Software Ltd.). Among the four different scoring functions available in the program, ASP [39],

ChemScore [40,41], GoldScore [42], and ChemPLP [43], the latter is claimed to be generally more effective than the other scoring functions for both pose prediction and virtual screening. ChemPLP is the default scoring function for GOLD 5.2 and was employed by us for the docking procedure.

Hydrogen atoms were added to protein structures based on ionization and tautomeric states defined by the program. Serine, threonine and tyrosine hydroxyl groups and lysine amino groups were free to rotate during the docking procedure to allow the best orientation of hydrogen bonds involving these groups. The number of genetic operations (crossover, migration, mutation) for each run was set to 100,000 during the searching procedure. The radius of the binding sites for the enzymes was set to 10 Å around atoms selected after superposition with available, related, ligand-containing crystallographic structures.

Acknowledgments

The authors would like to thank CNPq, FAPERJ, INCT-INOVAR, and CAPES for fellowship and financial support.

Appendix A. Supplementary data

Supplementary data related to this article can be found at <http://dx.doi.org/10.1016/j.ejmech.2015.06.014>.

References

- [1] WHO, Control of the Leishmaniases, 2010. World Health Organization Technical Report Series. Available: <http://www.pubmedcentral.nih.gov/articlerender.fcgi?artid=3307017&tool=pmcentrez&rendertype=abstract>.
- [2] L.H. Freitas-Junior, E. Chatelain, H.A. Kim, J.L. Siqueira-Neto, Visceral Leishmaniasis Treatment: what do we have, what do we need and how to deliver it? *Int. J. Parasitol.* 2 (2012) 11–19.
- [3] J. Alvar, I.D. Velez, C. Bern, M. Herrero, P. Desjeux, J. Cano, J. Jannin, M. Den Boer, Leishmaniasis worldwide and global estimates of its incidence, *PLoS ONE* 7 (2012) e35671.
- [4] L.F. Oliveira, A.O. Schubach, M.M. Martins, S.L. Passos, R.V. Oliveira, M.C. Marzochi, C.A. Andrade, Systematic review of the adverse effects of cutaneous Leishmaniasis treatment in the new world, *Acta Trop.* 118 (2011) 87–96.
- [5] F. Faraut-Gambarelli, R. Piarroux, M. Deniau, B. Giusiano, P. Marty, G. Michel, B. Faugère, H. Dumon, *In vitro* and *in vivo* resistance of *Leishmania infantum* to meglumine antimoniate: a study of 37 strains collected from patients with visceral Leishmaniasis, *Antimicrob. Agents Chemother.* 41 (1997) 827–830.
- [6] D.A. Goyeneche-Patino, L. Valderrama, J. Walker, N.G. Saravia, Antimony resistance and Trypanothione in experimentally selected and clinical strains of leishmania panamensis, *Antimicrob. Agents Chemother.* 52 (2008) 4503–4506.
- [7] H.C. Maltezou, Visceral Leishmaniasis: advances in treatment, *Recent Pat. Anti Infect Drug Discov.* 3 (2008) 192–198.
- [8] A.J.M. Nogueira, M.E.F. Lima, J.B.N. DaCosta, E.S.S. Alves, D.O. Anjos, M.A. Vannier-Santos, A.L. Rangel, Síntese, caracterização e estudo da atividade inibitória de novas dialquilfosforililidrazonas Sobre o crescimento de *Trypanosoma cruzi*, *Quím. Nova* 34 (2011) 1365–1369.
- [9] A. Montalvetti, B.N. Bailey, M.B. Martin, G.W. Severin, E. Oldfield, R. Docampo, Bisphosphonates are potent inhibitors of *Trypanosoma cruzi* Farnesyl pyrophosphate synthase, *J. Biol. Chem.* 276 (2001) 33930–33937.
- [10] V. Yardley, A.A. Khan, M.B. Martin, T.R. Slifer, F.G. Araujo, S.N.J. Moreno, R. Docampo, S.L. Croft, E. Oldfield, *In vivo* activities of farnesyl pyrophosphate synthase inhibitors against *Leishmania donovani* and *Toxoplasma gondii*, *Antimicrob. Agents Chemother.* 46 (2002) 929–931.
- [11] M.P. Hudock, C.E. Sanz-Rodríguez, Y. Song, J.M. Chan, Y. Zhang, S. Odeh, T. Kosztowski, A. Leon-Rossell, J.L. Concepción, V. Yardley, S.L. Croft, J.A. Urbina, E. Oldfield, Inhibition of *Trypanosoma cruzi* hexokinase by bisphosphonates, *J. Med. Chem.* 49 (2006) 215–223.
- [12] M.P. Barrett, The pentose phosphate pathway and parasitic protozoa, *Parasitol. Today* 13 (1997) 11–16.
- [13] D.A. Mauger, J.J. Cazzulo, R.J. Burchmore, M.P. Barrett, P.O. Ogbunode, Pentose phosphate metabolism in *Leishmania mexicana*, *Mol. Biochem. Parasit.* 130 (2003) 117–125.
- [14] W.O. Lin, M.C. Souza, J.B.N. DaCosta, Química de orqanofosforados. X: Síntese de *N*-dialquilfosforil-guanidinas, ureias e tioureas, *Quím. Nova* 18 (1995) 431–434.
- [15] J.M. Rodrigues, J.B.N. DaCosta, Synthesis and characterization of new symmetrical bisphosphonates, *Phosphorus Sulfur* 177 (2002) 137–149.

- [16] V.M.R. Dos Santos, J.B.N. DaCosta, C.M.R. Sant'anna, M.C.C. Oliveira, Synthesis, characterization, molecular modeling and biological activity against artemia salina of new symmetrical bisphosphoramidates, *Phosphorus Sulfur* 179 (2004) 173–184.
- [17] V.M.R. Dos Santos, C.M.R. Sant'anna, G.E.M. Borja, A. Chaaban, W.S. Côrtes, J.B.N. DaCosta, New bisphosphorothioates and bisphosphoroamidates: synthesis, molecular modeling and determination of insecticide and toxicological profile, *Bioorg. Chem.* 35 (2007) 68–81.
- [18] J.M. Rodrigues, C.M.R. Sant'anna, V.M. Rumjanek, J.B.N. DaCosta, Diastereoselective synthesis of new dialkylphosphorylhydrazones, *Phosphorus Sulfur* 185 (2010) 1–17.
- [19] L.C. Thomas, Interpretation of the Infrared Spectra of Organophosphorus Compounds, Heyden & Son, Ltd., London, 1974.
- [20] E. Pretsch, T. Clerc, J. Seibl, W. Simon, Tablas para la elucidacion estructural de compuestos organicos por metodos espectroscopicos, Madrid, Alhambra, 1980.
- [21] L.C. Thomas, The Identification of Functional Groups in Organophosphorus Compounds, first ed., Academic Press Inc. Ltd., London, 1974.
- [22] T. Mossmann, Rapid colorimetric assay for cellular growth and survival: application to proliferation and cytotoxicity assays, *J. Immunol. Methods* 65 (1983) 55–63.
- [23] J.C.M. Pereira, V. Caregaro, D.L. Costa, J. Santana Da Silva, F.Q. Cunha, D.W. Franco, Antileishmanial activity of ruthenium(II) tetraammine nitrosyl complexes, *Eur. J. Med. Chem.* 45 (2010) 4180–4187.
- [24] M. Biasini, S. Bienert, A. Waterhouse, K. Arnold, G. Studer, T. Schmidt, F. Kiefer, T.G. Cassarino, M. Bertoni, L. Bordoli, T. Schwede, SWISS-MODEL: modelling protein tertiary and quaternary structure using evolutionary information, *Nucleic Acids Res.* 42 (2014) W252–W258.
- [25] P. Benkert, M. Biasini, T. Schwede, Toward the estimation of the absolute quality of individual protein structure models, *Bioinformatics* 27 (2011) 343–350.
- [26] S.C. Lovell, I.W. Davis, W.B. Arendall III, de P.I.W. Bakker, J.M. Word, M.G. Prisant, J.S. Richardson, D.C. Richardson, Structure validation by α geometry: Φ , ψ and $C\beta$ deviation, *Proteins: Structure, Funct. Genet.* 50 (2002) 437–450.
- [27] W.F. Van Gunsteren, S.R. Billeter, A.A. Eising, P.H. Hünenberger, P. Krüger, A.E. Mark, W.R.P. Scott, I.G. Tironi, Biomolecular Simulation: the GROMOS96 Manual and User Guide, Vdf Hochschulverlag AG an der ETH, Zürich, Switzerland, 1996.
- [28] D. Rognan, Structure-based approaches to target fishing and ligand profiling, *Mol. Inf.* 29 (2010) 176–187.
- [29] J.L. Jenkins, A. Bender, J.W. Davies, *In Silico* target fishing: predicting biological targets from chemical structure, *Drug Discov. Today Technol.* 3 (2006) 413–421.
- [30] G.L. Warren, C.W. Andrews, A.M. Capelli, B. Clarke, J. Lalonde, M.H. Lambert, M. Lindvall, N. Nevins, S.F. Semus, S. Senger, G. Tedesco, I.D. Wall, J.M. Woolven, C.E. Peishoff, M.S. Head, A critical assessment of docking programs and scoring functions, *J. Med. Chem.* 49 (2006) 5912–5931.
- [31] C.E. Sanz-Rodríguez, J.L. Concepción, S. Pekerar, E. Oldfield, J. Urbina, Bisphosphonates as inhibitors of *Trypanosoma cruzi* hexokinase. Kinetic and metabolic studies, *J. Biol. Chem.* 282 (2007) 12377–12387.
- [32] X. Huang, W.A. Miller, Time-efficient, linear-space local similarity algorithm, *Adv. Appl. Math.* 12 (1991) 337–357.
- [33] A.I. Vogel, Análise Orgânica Qualitativa, Ao Livro Técnico S.A., RJ, 1981.
- [34] J.L. Ávila, A. Ávila, M.A. Polegre, V.E. Márquez, Specific inhibitory effect of 3-deazaneplanocin A against several *Leishmania mexicana* and *L. braziliensis* strains, *J. Trop. Med. Hyg.* 57 (1997) 407–412.
- [35] R.G. Titus, M. Marchand, T. Boon, J.A. Louis, A limiting dilution assay for quantifying *Leishmania major* in tissues of infected mice, *Parasite Immunol.* 7 (1985) 545–555.
- [36] N.E. Guex, M.C. Peitsch, SWISS-MODEL and the Swiss-Pdb viewer: an environment for comparative protein modeling, *Electrophoresis* 18 (1997) 2714–2723.
- [37] T. Schwede, J. Kopp, N. Guex, M.C. Peitsch, SWISS-MODEL: an automated protein homology-modeling server, *Nucleic Acids Res.* 31 (2003) 3381–3385.
- [38] J.J.P. Stewart, Optimization of parameters for semiempirical methods I, *Method. J. Comput. Chem.* 10 (1989) 209–220.
- [39] W.T. Mooij, M.L. Verdonk, General and targeted statistical potentials for protein-ligand interactions, *Proteins* 61 (2005) 272–287.
- [40] M.D. Eldridge, C.W. Murray, T.R. Auton, G.V. Paolini, R.P. Mee, Empirical scoring functions: I. The development of a fast empirical scoring function to estimate the binding affinity of ligands in receptor complexes, *J. Comput. Mol. Des.* 11 (1997) 425–445.
- [41] M.D. Eldridge, C.A. Baxter, C.W. Murray, D.E. Clark, D.R. Westhead, Flexible docking using tabu search and an empirical estimate of binding affinity, *Proteins* 33 (1998) 367–382.
- [42] G. Jones, P. Willett, R.C. Glen, A.R. Leach, R. Taylor, Development and validation of a genetic algorithm for flexible docking, *J. Mol. Biol.* 267 (1997) 727–748.
- [43] O. Korb, T. Stützle, T.E. Exner, empirical scoring functions for advanced protein-ligand docking with PLANTS, *J. Inf. Model* 49 (2009) 84–96.